A Supporting Materials

A.1 Further Discussion of the Reservoir State Method

In this section we provide additional information on the reservoir state method, including a more detailed mathematical treatment and a few more words on implementation.

We begin by partitioning the population distribution for each isomer into a low-energy *reservoir* and high-energy *active-state*. In our implementation we place the cutoff such that all of the reactive energies are in the active state, and none are in the reservoir. This differs from the suggestion of Green and Bhatti to place the cutoff a few $k_{\mathrm{B}}T$ below the lowest transition-state energy adjacent to that isomer.[32] The best choice of the cutoff likely varies from system to system and with both temperature and pressure; we have not tried to optimize this choice in this work.

The partitioned master equation (Equation (4)) for the isomers is

$$\frac{d}{dt}\begin{bmatrix}\mathbf{p}_1^{\mathrm{r}}\\ \mathbf{p}_1^{\mathrm{a}}\\ \mathbf{p}_2^{\mathrm{r}}\\ \mathbf{p}_2^{\mathrm{a}}\\ \vdots\end{bmatrix} = \begin{bmatrix}\mathbf{M}_1^{\mathrm{rr}} & \mathbf{M}_1^{\mathrm{ra}} & \mathbf{0} & \mathbf{0} & \dots\\ \mathbf{M}_1^{\mathrm{ar}} & \mathbf{M}_1^{\mathrm{aa}} & \mathbf{0} & \mathbf{K}_{12}^{\mathrm{a}} & \dots\\ \mathbf{0} & \mathbf{0} & \mathbf{M}_2^{\mathrm{rr}} & \mathbf{M}_2^{\mathrm{ra}} & \dots\\ \mathbf{0} & \mathbf{K}_{21}^{\mathrm{a}} & \mathbf{M}_2^{\mathrm{ar}} & \mathbf{M}_2^{\mathrm{aa}} & \dots\\ \vdots & \vdots & \vdots & \vdots & \ddots\end{bmatrix}\begin{bmatrix}\mathbf{p}_1^{\mathrm{r}}\\ \mathbf{p}_1^{\mathrm{a}}\\ \mathbf{p}_2^{\mathrm{r}}\\ \mathbf{p}_2^{\mathrm{a}}\\ \vdots\end{bmatrix} + \sum_{m=1}^{N_{\mathrm{reac}}} y_{m\mathrm{A}}y_{m\mathrm{B}}\begin{bmatrix}\mathbf{0}\\ \mathbf{F}_{1m}^{\mathrm{a}}\mathbf{b}_m^{\mathrm{a}}\\ \mathbf{0}\\ \mathbf{F}_{2m}^{\mathrm{a}}\mathbf{b}_m^{\mathrm{a}}\\ \vdots\end{bmatrix} \tag{45}$$

where $\mathbf{p}_i^{\mathrm{r}}$ and $\mathbf{p}_i^{\mathrm{a}}$ are the reservoir and active-state grains for isomer i, respectively. A Boltzmann distribution $\mathbf{b}_i^{\mathrm{r}}$ is imposed on the reservoir grains, i.e.

$$\mathbf{p}_i^{\mathrm{r}} = x_i(t)\mathbf{b}_i^{\mathrm{r}} \tag{46}$$

leaving a single time-dependent constant of proportionality $x_i(t)$ which is related to the total population of isomer i. The active-state grains are assumed to be in pseudo-steady state. The rows for the active-state grains are extracted and the pseudo-steady state approximation applied to give

$$\begin{bmatrix} \mathbf{0} \\ \mathbf{0} \\ \vdots \end{bmatrix} = \begin{bmatrix} \mathbf{M}_1^{\mathrm{aa}} & \mathbf{K}_{12}^{\mathrm{a}} & \cdots \\ \mathbf{K}_{21}^{\mathrm{a}} & \mathbf{M}_2^{\mathrm{aa}} & \cdots \\ \vdots & \vdots & \ddots \end{bmatrix} \begin{bmatrix} \mathbf{p}_1^{\mathrm{a}} \\ \mathbf{p}_2^{\mathrm{a}} \\ \vdots \end{bmatrix} + \begin{bmatrix} \mathbf{M}_1^{\mathrm{ar}} \mathbf{p}_1^{\mathrm{r}} \\ \mathbf{M}_2^{\mathrm{ar}} \mathbf{p}_2^{\mathrm{r}} \\ \vdots \end{bmatrix} + \sum_{m=1}^{N_{\mathrm{reac}}} y_{m\mathrm{A}} y_{m\mathrm{B}} \begin{bmatrix} \mathbf{F}_{1m}^{\mathrm{a}} \mathbf{b}_m^{\mathrm{a}} \\ \mathbf{F}_{2m}^{\mathrm{a}} \mathbf{b}_m^{\mathrm{a}} \\ \vdots \end{bmatrix} \tag{47}$$

After applying the reservoir state approximation, the active-state grain populations can be determined by a single linear solve of

$$\begin{bmatrix} \mathbf{M}_1^{\mathrm{aa}} & \mathbf{K}_{12}^{\mathrm{a}} & \cdots \\ \mathbf{K}_{21}^{\mathrm{a}} & \mathbf{M}_2^{\mathrm{aa}} & \cdots \\ \vdots & \vdots & \ddots \end{bmatrix} \begin{bmatrix} \mathbf{p}_1^{\mathrm{a}} \\ \mathbf{p}_2^{\mathrm{a}} \\ \vdots \end{bmatrix} = - \sum_{j=1}^{N_{\mathrm{isom}}} x_j \begin{bmatrix} \delta_{1j} \mathbf{M}_j^{\mathrm{ar}} \mathbf{b}_j^{\mathrm{r}} \\ \delta_{2j} \mathbf{M}_j^{\mathrm{ar}} \mathbf{b}_j^{\mathrm{r}} \\ \vdots \end{bmatrix} - \sum_{m=1}^{N_{\mathrm{reac}}} y_{m\mathrm{A}} y_{m\mathrm{B}} \begin{bmatrix} \mathbf{F}_{1m}^{\mathrm{a}} \mathbf{b}_m^{\mathrm{a}} \\ \mathbf{F}_{2m}^{\mathrm{a}} \mathbf{b}_m^{\mathrm{a}} \\ \vdots \end{bmatrix} \tag{48}$$

$$\mathbf{L}\mathbf{p}^{\mathrm{a}} = - \sum_{j=1}^{N_{\mathrm{isom}}} x_j \mathbf{z}_j - \sum_{m=1}^{N_{\mathrm{reac}}} y_{m\mathrm{A}} y_{m\mathrm{B}} \mathbf{w}_m \tag{49}$$

where δ_{ij} is the Kronecker delta. Only the jth block in each of the first set of right-hand side vectors is nonzero.

The solution procedure as given by Green and Bhatti is similar to the method presented in the previous section for the modified strong collision method, wherein an isomer or reactant channel is designated as the "entry" channel. The corresponding value of x_j or $y_{m\mathrm{A}} y_{m\mathrm{B}}$ is set to unity while all others are set to zero, which leaves exactly one of the right-hand side vectors from the equation above. Computing the steady-state vector then allows for determining the $k(T, P)$ values from the source to all other isomers, reactant channels, and product channels. Since the left-hand side matrix is independent of the choice of entry channel, we can again solve for the steady-state populations from each of the possible entry channels concurrently, i.e. one only needs to LU factorize the large matrix once. Furthermore, Equation (48) indicates that the true steady-state vector is a weighted sum of the steady-state vectors calculated for each source, where the weights are the isomer and reactant channel concentrations x_j and $y_{m\mathrm{A}} y_{m\mathrm{B}}$, as anticipated in Equation (24).

The pseudo-steady state values $\mathbf{p}_i^{\mathrm{a}}$ are given by

$$\mathbf{p}_i^{\mathrm{a}} = -\sum_{j=1}^{N_{\mathrm{isom}}} x_j \mathbf{Q}_{ij} \mathbf{M}_j^{\mathrm{ar}} \mathbf{b}_j^{\mathrm{r}} - \sum_{m=1}^{N_{\mathrm{reac}}} y_{m\mathrm{A}} y_{m\mathrm{B}} \sum_{j=1}^{N_{\mathrm{isom}}} \mathbf{Q}_{ij} \mathbf{F}_{jm}^{\mathrm{a}} \mathbf{b}_m^{\mathrm{a}} \tag{50}$$

where $\mathbf{Q} \equiv \mathbf{L}^{-1}$. The remaining reservoir-state grain ODEs are summed in the same way as the bimolecular well ODEs to give

$$\frac{dx_i}{dt} \sum_{s=1}^{N_{\mathrm{res},i}} (\mathbf{b}_i^{\mathrm{r}})_s = x_i \sum_{s=1}^{N_{\mathrm{res},i}} (\mathbf{M}_i^{\mathrm{rr}} \mathbf{b}_i^{\mathrm{r}})_s + \sum_{s=1}^{N_{\mathrm{res},i}} (\mathbf{M}_i^{\mathrm{ra}} \mathbf{p}_i^{\mathrm{a}})_s \tag{51}$$

$$\frac{dy_n}{dt} \sum_{s=1}^{N_{\mathrm{grains}}} (\mathbf{b}_n)_s = y_{n\mathrm{A}} y_{n\mathrm{B}} \sum_{s=1}^{N_{\mathrm{grains}}} (\mathbf{H}_n \mathbf{b}_n)_s + \sum_{i=1}^{N_{\mathrm{isom}}} \sum_{s=1}^{N_{\mathrm{grains}}} (\mathbf{G}_{mi}^{\mathrm{a}} \mathbf{p}_i^{\mathrm{a}})_s \tag{52}$$

Above we have introduced $N_{\mathrm{res},i}$ as the number of reservoir grains for isomer i. Substitution of Equation (50) above gives

$$\begin{aligned} \frac{dx_i}{dt} \sum_{s=1}^{N_{\mathrm{res},i}} (\mathbf{b}_i)_s &= x_i \sum_{s=1}^{N_{\mathrm{res},i}} (\mathbf{M}_i^{\mathrm{rr}} \mathbf{b}_i^{\mathrm{r}})_s - \sum_{j=1}^{N_{\mathrm{isom}}} x_j \sum_{s=1}^{N_{\mathrm{res},i}} \left(\mathbf{M}_i^{\mathrm{ra}} \mathbf{Q}_{ij} \mathbf{M}_j^{\mathrm{ar}} \mathbf{b}_j^{\mathrm{r}}\right)_s \\ &\quad - \sum_{m=1}^{N_{\mathrm{reac}}} y_{m\mathrm{A}} y_{m\mathrm{B}} \sum_{j=1}^{N_{\mathrm{isom}}} \sum_{s=1}^{N_{\mathrm{res},i}} \left(\mathbf{M}_i^{\mathrm{ra}} \mathbf{Q}_{ij} \mathbf{F}_{jm}^{\mathrm{a}} \mathbf{b}_m^{\mathrm{a}}\right)_s \end{aligned} \tag{53}$$

$$\begin{aligned} \frac{dy_n}{dt} \sum_{s=1}^{N_{\mathrm{grains}}} (\mathbf{b}_n)_s &= y_{n\mathrm{A}} y_{n\mathrm{B}} \sum_{s=1}^{N_{\mathrm{grains}}} (\mathbf{H}_n \mathbf{b}_n)_s - \sum_{j=1}^{N_{\mathrm{isom}}} x_j \sum_{i=1}^{N_{\mathrm{isom}}} \sum_{s=1}^{N_{\mathrm{grains}}} \left(\mathbf{G}_{ni}^{\mathrm{a}} \mathbf{Q}_{ij} \mathbf{M}_j^{\mathrm{ar}} \mathbf{b}_j^{\mathrm{r}}\right)_s \\ &\quad - \sum_{m=1}^{N_{\mathrm{reac}}} y_{m\mathrm{A}} y_{m\mathrm{B}} \sum_{i=1}^{N_{\mathrm{isom}}} \sum_{j=1}^{N_{\mathrm{isom}}} \sum_{s=1}^{N_{\mathrm{grains}}} \left(\mathbf{G}_{ni}^{\mathrm{a}} \mathbf{Q}_{ij} \mathbf{F}_{jm}^{\mathrm{a}} \mathbf{b}_m^{\mathrm{a}}\right)_s \end{aligned} \tag{54}$$

The left-hand sides of the above contain summations over normalized Boltzmann distributions. The summation in Equation (54) is for reactant channel n, and occurs over all energies; thus, since the Boltzmann distribution is normalized, by definition $\sum_{s=1}^{N_{\mathrm{grains}}} (b_n)_s = 1$. The summation in Equation (53) is for unimolecular isomer i, and occurs over only the low-energy grains that comprise the reservoir. At low temperatures the equilibrium distribution

is narrow, and therefore contained completely within the reservoir; in this limit the summation $\sum_{s=1}^{N_{\mathrm{res},i}} (b_i)_s \to 1$. However, at high temperatures there is significant population of the active-state grains at equilibrium, so the summation deviates from unity.

At this point we must decide on what we wish x_i to represent. Green and Bhatti designate it as the population of the reservoir only; in this case, the isomer equilibrium distributions must be renormalized to $\tilde{\mathbf{b}}_i$ such that $\sum_{s=1}^{N_{\mathrm{res},i}} (\tilde{b}_i)_s = 1$. For use in phenomenological kinetics equations, however, we would much rather have x_i represent the *total* population, including the excited active-state grains, so that the correct macroscopic equilibrium ratios are obtained. This is done by replacing $\sum_{s=1}^{N_{\mathrm{res},i}} (b_i)_s$ with $\sum_{s=1}^{N_{\mathrm{grains}}} (b_i)_s = 1$ on the left-hand side of Equation (53).

With the left-hand side summations set to unity, the phenomenological rate coefficients are given by

$$k_{ij}(T,P) = -\sum_{s=1}^{N_{\mathrm{res},i}} \left(\mathbf{M}_i^{\mathrm{ra}} \mathbf{Q}_{ij} \mathbf{M}_j^{\mathrm{ar}} \mathbf{b}_j^{\mathrm{r}}\right)_s \tag{55a}$$

$$k_{im}(T,P) = -\sum_{j=1}^{N_{\mathrm{isom}}} \sum_{s=1}^{N_{\mathrm{res},i}} \left(\mathbf{M}_i^{\mathrm{ra}} \mathbf{Q}_{ij} \mathbf{F}_{jm}^{\mathrm{a}} \mathbf{b}_m^{\mathrm{a}}\right)_s \tag{55b}$$

$$k_{nj}(T,P) = -\sum_{i=1}^{N_{\mathrm{isom}}} \sum_{s=1}^{N_{\mathrm{grains}}} \left(\mathbf{G}_{ni}^{\mathrm{a}} \mathbf{Q}_{ij} \mathbf{M}_j^{\mathrm{ar}} \mathbf{b}_j^{\mathrm{r}}\right)_s \tag{55c}$$

$$k_{nm}(T,P) = -\sum_{i=1}^{N_{\mathrm{isom}}} \sum_{j=1}^{N_{\mathrm{isom}}} \sum_{s=1}^{N_{\mathrm{grains}}} \left(\mathbf{G}_{ni}^{\mathrm{a}} \mathbf{Q}_{ij} \mathbf{F}_{jm}^{\mathrm{a}} \mathbf{b}_m^{\mathrm{a}}\right)_s \tag{55d}$$

which demonstrates that the rate constants $k(T,P)$ are independent of the initial condition. The indices above have the same meaning as in Equation (25): i and j represent unimolecular isomers, m represents bimolecular reactants, n represents bimolecular reactants and products, and s represents energy grains. The leading negative sign in each equation cancels with a negative produced from the matrix multiplication to give a positive value for the rate coefficient. The equations for k_{ij} and k_{im} involve summations over only the reservoir grains of

isomer i rather than all grains, which is a result of using the pseudo-steady state approximation on the active-state grains of isomer i.

The terms of the pseudo-steady state vector $\mathbf{p}_i^{\mathrm{a}}$ and the reservoir populations $\mathbf{b}_i^{\mathrm{r}}$ can be used to construct the $\mathbf{u}_{ij}$ and $\mathbf{v}_{im}$ vectors:

$$\mathbf{u}_{ij} = \begin{bmatrix} \delta_{ij}\mathbf{b}_j^{\mathrm{r}} \\ \mathbf{Q}_{ij}\mathbf{M}_j^{\mathrm{ar}}\mathbf{b}_j^{\mathrm{r}} \end{bmatrix} \qquad \mathbf{v}_{im} = \begin{bmatrix} \mathbf{0} \\ \sum_{j=1}^{N_{\mathrm{isom}}} \mathbf{Q}_{ij}\mathbf{F}_{jm}^{\mathrm{a}}\mathbf{b}_m^{\mathrm{a}} \end{bmatrix} \tag{56}$$

Again, using the above expressions with Equations (25) gives identical $k(T,P)$ values as those from Equations (36).

Finally, two notes on implementation. First, many of the terms of each summation over the isomers will be zero since many of the $\mathbf{G}_{ni}^{\mathrm{a}}$ and $\mathbf{F}_{jm}^{\mathrm{a}}$ matrices are zero. Second, it is more efficient to compute the vectors $\mathbf{Q}_{ij}\mathbf{M}_j^{\mathrm{ar}}\mathbf{b}_j^{\mathrm{r}}$ and $\mathbf{Q}_{ij}\mathbf{F}_{jm}^{\mathrm{a}}\mathbf{b}_m^{\mathrm{a}}$ than it is to compute the full active-state matrix inverse $\mathbf{Q}$. Our implementation of the reservoir state method takes advantage of both of these to accelerate the procedure.

A.2 Further Discussion of the Chemically-Significant Eigenvalues Method

This section presents the "initial-rate" method of converting chemically-significant eigenvalues and eigenvectors into phenomenological rate coefficients. The description and notation borrows significantly from the works of Miller and Klippenstein.[22,55,56]

The separation of the chemical and internal energy eigenvalues means that we can select a time after the initial energy modes have relaxed but before significant chemical transitions have occurred. After this induction period, the trajectory of the solution will be contained within the manifold defined by the chemically-significant eigenvectors. After the initial relaxation, the solution can be written in the form

$$\mathbf{p}(t) = \sum_{l=1}^{N_{\mathrm{chem}}} e^{\lambda_l t}\mathbf{x}_l\mathbf{z}_l^{\dagger}\mathbf{p}_0 = \sum_{l=1}^{N_{\mathrm{chem}}} e^{\lambda_l t}\mathbf{c}_l \tag{57}$$

where λ_l and $\mathbf{x}_l$ are the lth chemical eigenpair, $\mathbf{z}_l^\dagger$ is the corresponding row in $\mathbf{X}^{-1}$, and $\mathbf{p}_0$ is the initial condition. When $\mathbb{M}$ is symmetric, $\left(\mathbf{z}_l^\dagger\right)^{\mathrm{T}} = \mathbf{x}_l$.

By evaluating $\mathbf{p}(t)$ at $t = 0$ and $t \to \infty$, we observe that $\mathbf{c}_l^{(j)}$ contains the negative of the change in population of each energy grain for each isomer caused by relaxation of the lth chemical eigenmode and using isomer or reactant channel j as the entry point. It is conventional to use the initial conditions $\mathbf{p}_0^{(j)} = \mathbf{b}_j$ when computing $c_{irl}^{(j)}$; this assumes that each isomer could somehow individually be formed in a perfect Boltzmann energy distribution. If $c_{irl}^{(j)}$ is the entry in $\mathbf{c}_l^{(j)}$ corresponding to energy grain r for isomer i, then we can evaluate the total change in population $\Delta X_{il}^{(j)}$ by simply summing over the energy grains:

$$\Delta X_{il}^{(j)} = -\sum_{r=1}^{N_{\mathrm{grains}}} c_{irl}^{(j)} \tag{58}$$

There is only one entry in $\mathbf{c}_l^{(j)}$ for each bimolecular reactant channel n, so

$$\Delta X_{nl}^{(j)} = -c_{nl}^{(j)} \tag{59}$$

The value of $\Delta X_{ml}^{(j)}$ for bimolecular product channel m can also be evaluated from $\mathbf{c}_l^{(j)}$ via

$$\Delta X_{ml}^{(j)} = -\frac{1}{\lambda_l} \sum_{i=1}^{N_{\mathrm{isom}}} \sum_{r=1}^{N_{\mathrm{grains}}} (g_{mi})_r c_{irl}^{(j)} \tag{60}$$

where $(g_{mi})_r$ is the microcanonical rate for dissociation of isomer i to product channel m at energy grain r.

The $\Delta X_{il}^{(j)}$ can be directly related to the rate constants $k(T, P)$ that have isomer or reactant channel j as the reactant:

$$k_{ij}(T, P) = -\sum_{l=1}^{N_{\mathrm{chem}}} \lambda_l \Delta X_{il}^{(j)} \tag{61}$$

The index i in the above equation applies to isomers, reactants and products, while the index j applies to isomers or reactants.

Finally, the time-independent population distribution vector sets $\mathbf{u}_{ij}$ and $\mathbf{v}_{im}$ can be constructed directly from the chemically-significant eigenvectors:

$$u_{ij}(E_r) = \sum_{l=1}^{N_{\text{chem}}} c_{irl}^{(j)} \qquad v_{im}(E_r) = \sum_{l=1}^{N_{\text{chem}}} c_{irl}^{(m)} \tag{62}$$

A.3 Functional Group Characteristic Frequencies

Name	**Description**	**Mode**	**freq. range**	**# of modes**
RsCH3	5 atoms	C-H stretch	2750 - 2850	3
Alkane end group	1 rotor	R-C stretch	900 - 1100	1
	Terminal	R-C-H bend	1350 - 1500	2
		R-C-H rock	700 - 800	1
		R-C stretch	1000 - 1100	1
		Umbrella	1350 - 1400	1
RdCH2	4 atoms	C-H stretch	2950 - 3100	2
Alkene end group	no rotor	RdC stretch	1600 - 1700	1
	Terminal	R-C-H scissor	1330 - 1430	1
		R-C-H swing	900 - 1050	1
		R-C-H rock	1000 - 1050	1
CtCH	3 atoms	R-C-H bend	750 - 770	2
Alkyne end group	no rotor	C-H stretch	3350 - 3450	1
	Terminal	CtC stretch	2000 - 2200	
RsCH2sR	5 atoms	C-H stretch	2750 - 2850	2
saturated carbon with	2 rotors	H-C-H scissor	1425 - 1450	1
two single bonds	non-terminal	R-C-H symmetric	1225 - 1275	1
		R-C-H asymmetric	1270 - 1340	1
		H-C-H side rock	700 - 800	1

		R-C-R scissor	300 - 400	1
CdCHsR *carbon with double* *bond to carbon and* *single bond to R*	4 atoms 1 rotors non-terminal	C-H stretch R-C-H bend R-C-H bend CdC-R scissor CdC stretch	2995 - 3025 975 - 1000 1300 - 1375 400 - 500 1630 - 1680	1 1 1 1 1
Aldehyde *carbon with double* *bond to oxygen and* *single bond to R*	4 atoms 1 rotors non-terminal	C-H stretch R-C-H bend R-C-H bend OdC-R scissor R-C stretch OdC stretch	2695 - 2870 700 - 800 1380 - 1410 450 - 500 900 - 1100 1750 - 1800	1 1 1 1 1 1
Cumulene *carbon with two double* *bonds to carbon*	3 atoms no rotor non-terminal	C-C-C scissor C-C-C asymmetric stretch	540 - 610 1970 - 2140	2 1
Ketene *carbon with one carbon* *double bond and one* *oxygen double bond*	3 atoms no rotor non-terminal	OdC stretch OdCdC bend OdCdC bend	2110 - 2130 495 - 530 650 - 925	1 1 1
CtCsR *carbon with one* *triple bond and* *one single bond*	3 atoms 1 rotor non-terminal	CtC stretch CtC-C bend	2100 - 2250 500 - 550	1 1
RsCHsR2 *carbon with* *three single bonds*	5 atoms 3 rotors non-terminal	R-C-H bend C-C-C scissor C-H stretch	1380 - 1390 370 - 380 2800 - 3000	2 2 1

		Umbrella	430 0 440	1
CdCsR2	4 atoms	R-C-R scissor	325 - 375	1
carbon with one carbon	2 rotors	CdC-R scissor	415 - 465	1
double bond and two	non-terminal	Umbrella	420 - 450	1
single bonds		CdC stretch	1700 - 1750	1
Ketone	4 atoms	R-C-R scissor	365 - 385	1
carbon with one oxygen	2 rotors	OdC-R scissor	505 - 600	1
double bond and two	non-terminal	Umbrella	445 - 480	1
single bonds		OdC stretch	1700 - 1720	1
RsCsR3	5 atoms	C-C-C scissor	350 - 400	2
carbon with four	4 rotors	C-C-C bend	1190 - 1240	2
single bonds	non-terminal	Umbrella	400 - 500	1
RsCH2r	4 atoms	C-H stretch	3000 - 3100	2
carbon radical with	1 rotor	R-C-H swing	415 - 465	1
one single bond	terminal	R-C-H rock	780 - 850	1
		R-C stretch	900 - 1100	1
		R-C-H scissor	1435 - 1475	1
RdCHr	3 atoms	C-H stretch	3115 - 3125	1
carbon radical with	no rotors	CdC-H bend	620 - 680	1
one double bond	terminal	CdC stretch	1600 - 1700	1
		CdC-H bend	785 - 800	1
RsCHrsR	4 atoms	C-H stretch	3000 - 3050	1
carbon radical with	2 rotors	R-C-H bend	390 - 425	1
two single bonds	non-terminal	R-C-H bend	1340 - 1360	1
		R-C-R scissor	335 - 370	1
CdCrsR	3 atoms	CdC stretch	1670 - 1700	1
carbon radical with	1 rotor	CdC-R bend	300 - 440	1

one carbon double bond and one single bond	non-terminal			
OdCrsR *carbon radical with one oxygen double bond and one single bond*	3 atoms 1 rotor terminal	OdC stretch OdC-R bend R-C stretch	1850 - 1860 440 - 470 900 - 1100	1 1
RsCrsR2 *carbon radical with three single bonds*	4 atoms 3 rotors non-terminal	C-C-C scissor Umbrella	360 - 370 300 - 400	2 1
Alcohol *hydrogen bond and*	3 atoms terminal	O-H stretch R-O stretch R-O-H bend	3580 - 3650 900 - 1100 1210 - 1345	1 1 1
Ether *oxygen with two single carbon bonds*	3 atoms 2 rotors non-terminal	C-O-C scissor	350 - 500	1
ROOH	4 atoms terminal	O-H stretch O-O-H bend R-O stretch C-O-O scissor O-O stretch	3580 - 3650 1300 - 1320 900 - 1100 350 - 425 825 - 875	1 1 1 1 1
ROOR *peroxide*	4 atoms 3 rotors non-terminal	C-O-O scissor O-O stretch	350 - 500 795 - 815	1 1
peroxy radical	3 atoms terminal	C-O-O scissor C-O stretch O-O stretch	470 - 515 900 - 1100 1100 - 1170	1 1 1

Table 3: List of the functional groups and the corresponding frequency range for each vibrational mode.

A.4 Molecular Degrees of Freedom Using Various Methods

Table 4: Harmonic Oscillator Degrees of Freedom Using Various Methods

Species	Method	Frequency (degeneracy) (cm^{-1})
$CH_3C(=O)OO.$	Three frequency	467.3 (8), 1443.0 (7), 4069.3 (3)
	Group frequency	180.0 (3), 492.5, 750, 1000 (2), 1050, 1135, 1350, 1375, 1500, 2182.9, 2570, 2800, 2850
	Quantum chemistry	321.6, 503.5, 539.9, 547.1, 731.5, 979.2, 1044.0, 1126.4, 1188.6, 1399.4, 1458.2, 1463.4, 1881.7, 3055.3, 3115.4, 3155.1
$.CH_2C(=O)OOH$	Three frequency	391.4 (8), 1172.3 (7), 3800.5 (3)
	Group frequency	387.5, 420.1 (3), 440, 815, 850, 1000 (2), 1310, 1455, 1941.5, 3000, 3100, 3615
	Quantum chemistry	320.7, 423.4, 670.2, 680.0, 757.3, 869.8, 1004.4, 1025.6, 1243.6, 1446.5, 1494.6, 1698.0, 3164.2, 3282.4, 3454.9

Table 5: Hindered Rotor Degrees of Freedom Using Various Methods

Species	Method	(Frequency, Barrier height) (cm^{-1}, cm^{-1})
$CH_3C(=O)OO.$	Three frequency	n/a
	Group frequency	(502.3, 346.7), (677.7, 1637.4)
	Quantum chemistry	(139.4, 2139.3), (159.2, 425.8)
$.CH_2C(=O)OOH$	Three frequency	n/a
	Group frequency	(420.3, 1942.8), (1435.7, 1942.8), (420.3, 4772.1)
	Quantum chemistry	(336.8, 2189.5), (205.3, 5153.4), (321.9, 1672.3)
$CH_3C.=O$	Three frequency	n/a
	Group frequency	(600.0, 1041.7)
	Quantum chemistry	(112.4, 176.4)

A.5 Other Calculated Quantities

Densities of States for Isomers and Reactants in Acetyl + O_2 Network

The following values were computed from quantum chemistry calculations using density functional theory (specifically the B3LYP method), with a hindered rotor treatment.

Energy (kcal/mol)	Acetylperoxy (cm^{-1})	Hydroperoxylvinoxy (cm^{-1})	Acetyl + O_2 (cm^{-1})
0.0	0.000e+00	0.000e+00	0.000e+00
0.5	0.000e+00	0.000e+00	0.000e+00
1.0	8.474e-04	0.000e+00	0.000e+00
1.5	2.428e-03	0.000e+00	0.000e+00
2.0	5.896e-03	0.000e+00	0.000e+00
2.5	1.165e-02	0.000e+00	0.000e+00
3.0	2.487e-02	1.484e-04	0.000e+00
3.5	4.579e-02	5.586e-04	0.000e+00
4.0	7.964e-02	1.522e-03	0.000e+00
4.5	1.356e-01	3.549e-03	0.000e+00
5.0	2.215e-01	7.407e-03	0.000e+00
5.5	3.545e-01	1.479e-02	0.000e+00
6.0	5.583e-01	2.746e-02	0.000e+00
6.5	8.519e-01	4.925e-02	0.000e+00
7.0	1.288e+00	8.493e-02	0.000e+00
7.5	1.914e+00	1.426e-01	0.000e+00
8.0	2.787e+00	2.334e-01	0.000e+00
8.5	4.024e+00	3.726e-01	0.000e+00
9.0	5.735e+00	5.833e-01	0.000e+00
9.5	8.070e+00	8.964e-01	0.000e+00
10.0	1.126e+01	1.356e+00	0.000e+00
10.5	1.555e+01	2.020e+00	0.000e+00
11.0	2.128e+01	2.969e+00	0.000e+00
11.5	2.890e+01	4.308e+00	0.000e+00
12.0	3.891e+01	6.180e+00	0.000e+00
12.5	5.202e+01	8.771e+00	0.000e+00
13.0	6.911e+01	1.233e+01	0.000e+00
13.5	9.117e+01	1.716e+01	0.000e+00
14.0	1.195e+02	2.369e+01	0.000e+00
14.5	1.558e+02	3.243e+01	0.000e+00
15.0	2.020e+02	4.405e+01	0.000e+00
15.5	2.605e+02	5.940e+01	0.000e+00
16.0	3.344e+02	7.956e+01	0.000e+00
16.5	4.270e+02	1.059e+02	0.000e+00
17.0	5.428e+02	1.400e+02	0.000e+00
17.5	6.872e+02	1.840e+02	0.000e+00
18.0	8.661e+02	2.406e+02	0.000e+00
18.5	1.087e+03	3.129e+02	0.000e+00
19.0	1.360e+03	4.048e+02	0.000e+00
19.5	1.695e+03	5.212e+02	0.000e+00
20.0	2.104e+03	6.679e+02	0.000e+00
20.5	2.603e+03	8.521e+02	0.000e+00
21.0	3.211e+03	1.082e+03	0.000e+00
21.5	3.947e+03	1.369e+03	0.000e+00
22.0	4.837e+03	1.726e+03	0.000e+00
22.5	5.911e+03	2.166e+03	0.000e+00
23.0	7.202e+03	2.709e+03	0.000e+00
23.5	8.751e+03	3.377e+03	0.000e+00
24.0	1.060e+04	4.194e+03	0.000e+00
24.5	1.282e+04	5.192e+03	0.000e+00
25.0	1.545e+04	6.408e+03	0.000e+00
25.5	1.858e+04	7.883e+03	0.000e+00

26.0	2.229e+04	9.670e+03	0.000e+00
26.5	2.669e+04	1.183e+04	0.000e+00
27.0	3.187e+04	1.443e+04	0.000e+00
27.5	3.798e+04	1.755e+04	0.000e+00
28.0	4.516e+04	2.129e+04	0.000e+00
28.5	5.360e+04	2.576e+04	0.000e+00
29.0	6.348e+04	3.110e+04	0.000e+00
29.5	7.503e+04	3.745e+04	0.000e+00
30.0	8.851e+04	4.500e+04	0.000e+00
30.5	1.042e+05	5.394e+04	0.000e+00
31.0	1.225e+05	6.452e+04	0.000e+00
31.5	1.437e+05	7.701e+04	0.000e+00
32.0	1.684e+05	9.172e+04	0.000e+00
32.5	1.969e+05	1.090e+05	0.000e+00
33.0	2.298e+05	1.293e+05	0.000e+00
33.5	2.679e+05	1.531e+05	0.000e+00
34.0	3.117e+05	1.809e+05	0.000e+00
34.5	3.622e+05	2.134e+05	0.000e+00
35.0	4.202e+05	2.513e+05	0.000e+00
35.5	4.868e+05	2.954e+05	0.000e+00
36.0	5.631e+05	3.466e+05	2.178e-02
36.5	6.505e+05	4.059e+05	8.308e-02
37.0	7.503e+05	4.747e+05	1.283e-01
37.5	8.644e+05	5.543e+05	1.980e-01
38.0	9.944e+05	6.462e+05	2.893e-01
38.5	1.143e+06	7.521e+05	3.889e-01
39.0	1.311e+06	8.742e+05	6.100e-01
39.5	1.503e+06	1.014e+06	8.872e-01
40.0	1.720e+06	1.176e+06	1.200e+00
40.5	1.967e+06	1.361e+06	1.742e+00
41.0	2.246e+06	1.572e+06	2.316e+00
41.5	2.562e+06	1.814e+06	3.129e+00
42.0	2.919e+06	2.091e+06	4.259e+00
42.5	3.322e+06	2.407e+06	5.451e+00
43.0	3.776e+06	2.767e+06	7.117e+00
43.5	4.288e+06	3.177e+06	9.243e+00
44.0	4.865e+06	3.643e+06	1.170e+01
44.5	5.513e+06	4.173e+06	1.510e+01
45.0	6.241e+06	4.774e+06	1.914e+01
45.5	7.059e+06	5.455e+06	2.402e+01
46.0	7.975e+06	6.226e+06	3.020e+01
46.5	9.003e+06	7.099e+06	3.735e+01
47.0	1.015e+07	8.085e+06	4.614e+01
47.5	1.144e+07	9.197e+06	5.699e+01
48.0	1.287e+07	1.045e+07	6.966e+01
48.5	1.448e+07	1.187e+07	8.520e+01
49.0	1.627e+07	1.346e+07	1.037e+02
49.5	1.826e+07	1.525e+07	1.254e+02
50.0	2.049e+07	1.726e+07	1.514e+02
50.5	2.296e+07	1.951e+07	1.821e+02
51.0	2.571e+07	2.204e+07	2.180e+02
51.5	2.876e+07	2.487e+07	2.606e+02
52.0	3.216e+07	2.805e+07	3.101e+02
52.5	3.592e+07	3.159e+07	3.679e+02
53.0	4.010e+07	3.556e+07	4.358e+02
53.5	4.472e+07	3.999e+07	5.144e+02
54.0	4.984e+07	4.492e+07	6.059e+02
54.5	5.550e+07	5.043e+07	7.119e+02
55.0	6.177e+07	5.656e+07	8.337e+02
55.5	6.868e+07	6.339e+07	9.744e+02
56.0	7.632e+07	7.098e+07	1.136e+03
56.5	8.475e+07	7.942e+07	1.322e+03
57.0	9.405e+07	8.879e+07	1.535e+03
57.5	1.043e+08	9.918e+07	1.778e+03
58.0	1.156e+08	1.107e+08	2.056e+03

58.5	1.280e+08	1.235e+08	2.374e+03
59.0	1.416e+08	1.376e+08	2.734e+03
59.5	1.566e+08	1.533e+08	3.144e+03
60.0	1.731e+08	1.706e+08	3.609e+03
60.5	1.912e+08	1.897e+08	4.135e+03
61.0	2.111e+08	2.108e+08	4.730e+03
61.5	2.328e+08	2.341e+08	5.401e+03
62.0	2.567e+08	2.598e+08	6.159e+03
62.5	2.828e+08	2.882e+08	7.013e+03
63.0	3.115e+08	3.194e+08	7.972e+03
63.5	3.428e+08	3.537e+08	9.049e+03
64.0	3.770e+08	3.915e+08	1.026e+04
64.5	4.144e+08	4.331e+08	1.161e+04
65.0	4.553e+08	4.787e+08	1.312e+04
65.5	5.000e+08	5.289e+08	1.481e+04
66.0	5.487e+08	5.839e+08	1.670e+04
66.5	6.018e+08	6.442e+08	1.880e+04
67.0	6.597e+08	7.104e+08	2.115e+04
67.5	7.228e+08	7.828e+08	2.375e+04
68.0	7.916e+08	8.622e+08	2.665e+04
68.5	8.664e+08	9.491e+08	2.986e+04
69.0	9.478e+08	1.044e+09	3.343e+04
69.5	1.036e+09	1.148e+09	3.738e+04
70.0	1.133e+09	1.261e+09	4.175e+04
70.5	1.237e+09	1.385e+09	4.658e+04
71.0	1.351e+09	1.521e+09	5.192e+04
71.5	1.474e+09	1.668e+09	5.780e+04
72.0	1.608e+09	1.829e+09	6.430e+04
72.5	1.753e+09	2.005e+09	7.145e+04
73.0	1.910e+09	2.196e+09	7.932e+04
73.5	2.080e+09	2.404e+09	8.798e+04
74.0	2.265e+09	2.630e+09	9.749e+04
74.5	2.465e+09	2.876e+09	1.079e+05
75.0	2.681e+09	3.144e+09	1.194e+05
75.5	2.915e+09	3.435e+09	1.319e+05
76.0	3.168e+09	3.751e+09	1.457e+05
76.5	3.441e+09	4.094e+09	1.608e+05
77.0	3.737e+09	4.467e+09	1.772e+05
77.5	4.056e+09	4.871e+09	1.952e+05
78.0	4.400e+09	5.309e+09	2.149e+05
78.5	4.772e+09	5.784e+09	2.363e+05
79.0	5.173e+09	6.298e+09	2.597e+05
79.5	5.605e+09	6.856e+09	2.851e+05
80.0	6.071e+09	7.459e+09	3.129e+05
80.5	6.574e+09	8.111e+09	3.431e+05
81.0	7.115e+09	8.817e+09	3.759e+05
81.5	7.698e+09	9.580e+09	4.116e+05
82.0	8.325e+09	1.040e+10	4.504e+05
82.5	8.999e+09	1.130e+10	4.925e+05
83.0	9.725e+09	1.226e+10	5.381e+05
83.5	1.051e+10	1.330e+10	5.876e+05
84.0	1.134e+10	1.442e+10	6.413e+05
84.5	1.225e+10	1.562e+10	6.993e+05
85.0	1.321e+10	1.693e+10	7.622e+05
85.5	1.425e+10	1.833e+10	8.302e+05
86.0	1.537e+10	1.984e+10	9.037e+05
86.5	1.657e+10	2.147e+10	9.831e+05
87.0	1.785e+10	2.323e+10	1.069e+06
87.5	1.923e+10	2.512e+10	1.161e+06
88.0	2.071e+10	2.715e+10	1.261e+06
88.5	2.229e+10	2.933e+10	1.369e+06
89.0	2.398e+10	3.168e+10	1.485e+06
89.5	2.580e+10	3.420e+10	1.610e+06
90.0	2.774e+10	3.691e+10	1.745e+06
90.5	2.982e+10	3.982e+10	1.889e+06

91.0	3.205e+10	4.295e+10	2.045e+06
91.5	3.443e+10	4.630e+10	2.213e+06
92.0	3.698e+10	4.990e+10	2.392e+06
92.5	3.970e+10	5.376e+10	2.586e+06
93.0	4.261e+10	5.790e+10	2.793e+06
93.5	4.572e+10	6.234e+10	3.016e+06
94.0	4.904e+10	6.709e+10	3.254e+06
94.5	5.258e+10	7.218e+10	3.510e+06
95.0	5.637e+10	7.763e+10	3.784e+06
95.5	6.041e+10	8.347e+10	4.078e+06
96.0	6.472e+10	8.971e+10	4.393e+06
96.5	6.932e+10	9.640e+10	4.729e+06
97.0	7.422e+10	1.035e+11	5.089e+06
97.5	7.944e+10	1.112e+11	5.475e+06
98.0	8.501e+10	1.194e+11	5.886e+06
98.5	9.095e+10	1.281e+11	6.326e+06
99.0	9.727e+10	1.374e+11	6.796e+06
99.5	1.040e+11	1.474e+11	7.297e+06
100.0	1.112e+11	1.580e+11	7.833e+06
100.5	1.188e+11	1.693e+11	8.404e+06
101.0	1.269e+11	1.814e+11	9.013e+06
101.5	1.355e+11	1.943e+11	9.663e+06
102.0	1.447e+11	2.081e+11	1.035e+07
102.5	1.545e+11	2.228e+11	1.109e+07
103.0	1.649e+11	2.385e+11	1.188e+07
103.5	1.759e+11	2.551e+11	1.271e+07
104.0	1.876e+11	2.729e+11	1.360e+07
104.5	2.001e+11	2.918e+11	1.455e+07
105.0	2.133e+11	3.120e+11	1.556e+07
105.5	2.273e+11	3.334e+11	1.662e+07
106.0	2.422e+11	3.562e+11	1.776e+07
106.5	2.581e+11	3.805e+11	1.897e+07
107.0	2.748e+11	4.063e+11	2.025e+07
107.5	2.926e+11	4.338e+11	2.161e+07
108.0	3.115e+11	4.630e+11	2.306e+07
108.5	3.315e+11	4.940e+11	2.459e+07
109.0	3.527e+11	5.270e+11	2.622e+07
109.5	3.752e+11	5.620e+11	2.795e+07
110.0	3.991e+11	5.992e+11	2.978e+07
110.5	4.243e+11	6.387e+11	3.171e+07
111.0	4.510e+11	6.806e+11	3.377e+07
111.5	4.793e+11	7.251e+11	3.594e+07
112.0	5.093e+11	7.723e+11	3.824e+07
112.5	5.410e+11	8.224e+11	4.068e+07
113.0	5.746e+11	8.755e+11	4.326e+07
113.5	6.101e+11	9.318e+11	4.599e+07
114.0	6.477e+11	9.915e+11	4.887e+07
114.5	6.874e+11	1.055e+12	5.192e+07
115.0	7.294e+11	1.122e+12	5.515e+07
115.5	7.738e+11	1.193e+12	5.856e+07
116.0	8.207e+11	1.268e+12	6.216e+07
116.5	8.703e+11	1.348e+12	6.596e+07
117.0	9.227e+11	1.432e+12	6.997e+07
117.5	9.781e+11	1.521e+12	7.421e+07
118.0	1.036e+12	1.616e+12	7.868e+07
118.5	1.098e+12	1.716e+12	8.340e+07
119.0	1.163e+12	1.822e+12	8.838e+07
119.5	1.232e+12	1.933e+12	9.363e+07
120.0	1.305e+12	2.052e+12	9.916e+07
120.5	1.381e+12	2.176e+12	1.050e+08
121.0	1.462e+12	2.309e+12	1.111e+08
121.5	1.547e+12	2.448e+12	1.176e+08
122.0	1.637e+12	2.596e+12	1.244e+08
122.5	1.732e+12	2.751e+12	1.316e+08
123.0	1.831e+12	2.916e+12	1.392e+08

123.5	1.937e+12	3.089e+12	1.471e+08
124.0	2.047e+12	3.273e+12	1.555e+08
124.5	2.164e+12	3.466e+12	1.643e+08
125.0	2.287e+12	3.671e+12	1.736e+08
125.5	2.417e+12	3.886e+12	1.833e+08
126.0	2.553e+12	4.113e+12	1.936e+08
126.5	2.697e+12	4.353e+12	2.043e+08
127.0	2.848e+12	4.606e+12	2.156e+08
127.5	3.007e+12	4.872e+12	2.275e+08
128.0	3.174e+12	5.153e+12	2.400e+08
128.5	3.350e+12	5.449e+12	2.531e+08
129.0	3.536e+12	5.760e+12	2.669e+08
129.5	3.730e+12	6.089e+12	2.813e+08
130.0	3.935e+12	6.435e+12	2.965e+08
130.5	4.151e+12	6.799e+12	3.124e+08
131.0	4.377e+12	7.183e+12	3.291e+08
131.5	4.615e+12	7.587e+12	3.466e+08
132.0	4.865e+12	8.012e+12	3.649e+08
132.5	5.128e+12	8.459e+12	3.842e+08
133.0	5.404e+12	8.930e+12	4.044e+08
133.5	5.694e+12	9.425e+12	4.255e+08
134.0	5.998e+12	9.946e+12	4.477e+08
134.5	6.318e+12	1.049e+13	4.709e+08
135.0	6.653e+12	1.107e+13	4.952e+08
135.5	7.006e+12	1.167e+13	5.207e+08
136.0	7.375e+12	1.231e+13	5.473e+08
136.5	7.763e+12	1.298e+13	5.752e+08
137.0	8.171e+12	1.368e+13	6.045e+08
137.5	8.598e+12	1.442e+13	6.350e+08
138.0	9.046e+12	1.520e+13	6.670e+08
138.5	9.515e+12	1.601e+13	7.005e+08
139.0	1.001e+13	1.687e+13	7.355e+08
139.5	1.052e+13	1.776e+13	7.721e+08
140.0	1.107e+13	1.871e+13	8.103e+08
140.5	1.163e+13	1.970e+13	8.503e+08
141.0	1.223e+13	2.074e+13	8.921e+08
141.5	1.285e+13	2.182e+13	9.358e+08
142.0	1.350e+13	2.297e+13	9.815e+08
142.5	1.419e+13	2.417e+13	1.029e+09
143.0	1.490e+13	2.542e+13	1.079e+09
143.5	1.565e+13	2.674e+13	1.131e+09
144.0	1.644e+13	2.813e+13	1.185e+09
144.5	1.726e+13	2.958e+13	1.242e+09
145.0	1.812e+13	3.110e+13	1.301e+09
145.5	1.903e+13	3.269e+13	1.363e+09
146.0	1.997e+13	3.436e+13	1.427e+09
146.5	2.096e+13	3.610e+13	1.495e+09
147.0	2.199e+13	3.794e+13	1.565e+09
147.5	2.307e+13	3.985e+13	1.638e+09
148.0	2.420e+13	4.186e+13	1.714e+09
148.5	2.538e+13	4.397e+13	1.794e+09
149.0	2.661e+13	4.617e+13	1.876e+09
149.5	2.791e+13	4.847e+13	1.963e+09
150.0	2.926e+13	5.089e+13	2.053e+09
150.5	3.067e+13	5.341e+13	2.147e+09
151.0	3.214e+13	5.605e+13	2.244e+09
151.5	3.369e+13	5.882e+13	2.346e+09
152.0	3.530e+13	6.171e+13	2.452e+09
152.5	3.698e+13	6.474e+13	2.563e+09
153.0	3.874e+13	6.790e+13	2.678e+09
153.5	4.058e+13	7.121e+13	2.797e+09
154.0	4.249e+13	7.467e+13	2.922e+09
154.5	4.450e+13	7.828e+13	3.052e+09
155.0	4.659e+13	8.206e+13	3.187e+09
155.5	4.877e+13	8.601e+13	3.327e+09

156.0	5.105e+13	9.014e+13	3.473e+09
156.5	5.343e+13	9.446e+13	3.625e+09
157.0	5.591e+13	9.896e+13	3.783e+09
157.5	5.850e+13	1.037e+14	3.948e+09
158.0	6.121e+13	1.086e+14	4.119e+09
158.5	6.403e+13	1.137e+14	4.296e+09
159.0	6.697e+13	1.191e+14	4.481e+09
159.5	7.004e+13	1.247e+14	4.673e+09
160.0	7.324e+13	1.305e+14	4.873e+09

Microcanonical Rate Coefficients for Path Reactions in Acetyl + O_2 Network

$$\mathrm{CH_3CO + O_2} \overset{k_1}{\rightleftharpoons} \mathrm{CH_3C(O)OO}$$

$$\mathrm{CH_3C(O)OO} \overset{k_2}{\rightleftharpoons} \mathrm{CH_2C(O)OOH}$$

$$\mathrm{CH_3C(O)OO} \overset{k_3}{\rightleftharpoons} \mathrm{CH_2CO + HO_2}$$

$$\mathrm{CH_2C(O)OOH} \overset{k_4}{\rightleftharpoons} \mathrm{CH_2CO + HO_2}$$

$$\mathrm{CH_2C(O)OOH} \overset{k_5}{\rightleftharpoons} \mathrm{lactone + OH}$$

Energy (kcal/mol)	$k_1(E)$ (cm^3/mol·s)	$k_2(E)$ (s^{-1})	$k_3(E)$ (s^{-1})	$k_4(E)$ (s^{-1})	$k_5(E)$ (s^{-1})
-34.6	0.000e+00	0.000e+00	0.000e+00	0.000e+00	0.000e+00
-34.3	0.000e+00	0.000e+00	0.000e+00	0.000e+00	0.000e+00
-33.7	0.000e+00	0.000e+00	0.000e+00	0.000e+00	0.000e+00
-33.2	0.000e+00	0.000e+00	0.000e+00	0.000e+00	0.000e+00
-32.6	0.000e+00	0.000e+00	0.000e+00	0.000e+00	0.000e+00
-32.0	0.000e+00	4.610e-16	0.000e+00	0.000e+00	0.000e+00
-31.5	0.000e+00	1.780e-14	0.000e+00	0.000e+00	0.000e+00
-30.9	0.000e+00	2.260e-13	0.000e+00	0.000e+00	0.000e+00
-30.3	0.000e+00	1.790e-12	0.000e+00	0.000e+00	6.460e-50
-29.7	0.000e+00	1.100e-11	0.000e+00	0.000e+00	3.740e-46
-29.2	0.000e+00	5.600e-11	0.000e+00	0.000e+00	3.320e-43
-28.6	0.000e+00	2.500e-10	0.000e+00	0.000e+00	1.090e-40
-28.0	0.000e+00	1.010e-09	0.000e+00	0.000e+00	1.930e-38
-27.4	0.000e+00	3.720e-09	0.000e+00	0.000e+00	2.130e-36
-26.9	0.000e+00	1.280e-08	0.000e+00	0.000e+00	1.680e-34
-26.3	0.000e+00	4.180e-08	0.000e+00	0.000e+00	9.920e-33
-25.7	0.000e+00	1.290e-07	0.000e+00	0.000e+00	4.670e-31
-25.2	0.000e+00	3.820e-07	0.000e+00	0.000e+00	1.800e-29
-24.6	0.000e+00	1.090e-06	0.000e+00	0.000e+00	5.910e-28
-24.0	0.000e+00	2.990e-06	0.000e+00	0.000e+00	1.670e-26
-23.4	0.000e+00	7.950e-06	0.000e+00	0.000e+00	4.170e-25
-22.9	0.000e+00	2.060e-05	0.000e+00	0.000e+00	9.240e-24
-22.3	0.000e+00	5.190e-05	0.000e+00	0.000e+00	1.860e-22
-21.7	0.000e+00	1.280e-04	0.000e+00	0.000e+00	3.390e-21
-21.2	0.000e+00	3.080e-04	0.000e+00	0.000e+00	5.710e-20
-20.6	0.000e+00	7.260e-04	0.000e+00	0.000e+00	8.870e-19
-20.0	0.000e+00	1.680e-03	0.000e+00	0.000e+00	1.290e-17
-19.4	0.000e+00	3.840e-03	0.000e+00	0.000e+00	1.740e-16
-18.9	0.000e+00	8.600e-03	0.000e+00	0.000e+00	2.240e-15
-18.3	0.000e+00	1.900e-02	0.000e+00	0.000e+00	2.690e-14
-17.7	0.000e+00	4.130e-02	0.000e+00	0.000e+00	3.090e-13

-17.2	0.000e+00	8.860e-02	0.000e+00	0.000e+00	3.360e-12
-16.6	0.000e+00	1.880e-01	0.000e+00	0.000e+00	3.500e-11
-16.0	0.000e+00	3.930e-01	0.000e+00	0.000e+00	3.490e-10
-15.4	0.000e+00	8.150e-01	0.000e+00	0.000e+00	3.330e-09
-14.9	0.000e+00	1.670e+00	0.000e+00	0.000e+00	3.060e-08
-14.3	0.000e+00	3.380e+00	0.000e+00	0.000e+00	2.710e-07
-13.7	0.000e+00	6.790e+00	0.000e+00	0.000e+00	2.320e-06
-13.2	0.000e+00	1.350e+01	0.000e+00	0.000e+00	1.920e-05
-12.6	0.000e+00	2.660e+01	0.000e+00	0.000e+00	1.540e-04
-12.0	0.000e+00	5.200e+01	0.000e+00	0.000e+00	1.190e-03
-11.4	0.000e+00	1.010e+02	0.000e+00	0.000e+00	9.030e-03
-10.9	0.000e+00	1.940e+02	0.000e+00	0.000e+00	6.620e-02
-10.3	0.000e+00	3.700e+02	0.000e+00	0.000e+00	4.740e-01
-9.7	0.000e+00	7.000e+02	0.000e+00	0.000e+00	3.300e+00
-9.1	0.000e+00	1.320e+03	0.000e+00	0.000e+00	2.240e+01
-8.6	0.000e+00	2.450e+03	0.000e+00	0.000e+00	1.490e+02
-8.0	0.000e+00	4.540e+03	0.000e+00	0.000e+00	9.550e+02
-7.4	0.000e+00	8.320e+03	0.000e+00	0.000e+00	5.670e+03
-6.9	0.000e+00	1.510e+04	0.000e+00	0.000e+00	2.740e+04
-6.3	0.000e+00	2.680e+04	4.170e-07	1.320e-03	1.020e+05
-5.7	0.000e+00	4.650e+04	3.790e-05	5.750e-01	2.990e+05
-5.1	0.000e+00	7.870e+04	6.810e-04	3.620e+01	7.360e+05
-4.6	0.000e+00	1.290e+05	6.790e-03	8.790e+02	1.580e+06
-4.0	0.000e+00	2.060e+05	4.890e-02	7.070e+03	3.070e+06
-3.4	0.000e+00	3.190e+05	2.850e-01	2.960e+04	5.510e+06
-2.9	0.000e+00	4.830e+05	1.430e+00	8.660e+04	9.310e+06
-2.3	0.000e+00	7.120e+05	6.340e+00	2.070e+05	1.500e+07
-1.7	0.000e+00	1.030e+06	2.570e+01	4.320e+05	2.320e+07
-1.1	0.000e+00	1.450e+06	9.630e+01	8.190e+05	3.460e+07
-0.6	0.000e+00	2.020e+06	3.360e+02	1.440e+06	5.000e+07
0.0	2.650e+12	2.760e+06	1.090e+03	2.390e+06	7.060e+07
0.6	2.650e+12	3.710e+06	3.220e+03	3.780e+06	9.730e+07
1.1	2.650e+12	4.920e+06	8.520e+03	5.750e+06	1.320e+08
1.7	2.650e+12	6.440e+06	2.010e+04	8.470e+06	1.750e+08
2.3	2.650e+12	8.330e+06	4.290e+04	1.210e+07	2.280e+08
2.9	2.650e+12	1.070e+07	8.430e+04	1.690e+07	2.930e+08
3.4	2.650e+12	1.350e+07	1.550e+05	2.310e+07	3.720e+08
4.0	2.650e+12	1.690e+07	2.700e+05	3.090e+07	4.670e+08
4.6	2.650e+12	2.100e+07	4.480e+05	4.080e+07	5.790e+08
5.1	2.650e+12	2.590e+07	7.170e+05	5.290e+07	7.110e+08
5.7	2.650e+12	3.170e+07	1.110e+06	6.760e+07	8.650e+08
6.3	2.650e+12	3.850e+07	1.670e+06	8.540e+07	1.040e+09
6.9	2.650e+12	4.640e+07	2.450e+06	1.070e+08	1.250e+09
7.4	2.650e+12	5.570e+07	3.510e+06	1.320e+08	1.480e+09
8.0	2.650e+12	6.630e+07	4.940e+06	1.610e+08	1.750e+09
8.6	2.650e+12	7.850e+07	6.820e+06	1.950e+08	2.050e+09
9.1	2.650e+12	9.250e+07	9.260e+06	2.350e+08	2.380e+09
9.7	2.650e+12	1.080e+08	1.240e+07	2.800e+08	2.760e+09
10.3	2.650e+12	1.270e+08	1.640e+07	3.320e+08	3.170e+09
10.9	2.650e+12	1.470e+08	2.140e+07	3.910e+08	3.640e+09
11.4	2.650e+12	1.700e+08	2.760e+07	4.570e+08	4.140e+09
12.0	2.650e+12	1.960e+08	3.520e+07	5.320e+08	4.700e+09
12.6	2.650e+12	2.240e+08	4.460e+07	6.150e+08	5.320e+09
13.2	2.650e+12	2.570e+08	5.580e+07	7.080e+08	5.980e+09
13.7	2.650e+12	2.920e+08	6.940e+07	8.120e+08	6.710e+09
14.3	2.650e+12	3.320e+08	8.560e+07	9.260e+08	7.500e+09
14.9	2.650e+12	3.750e+08	1.050e+08	1.050e+09	8.350e+09
15.4	2.650e+12	4.230e+08	1.270e+08	1.190e+09	9.270e+09
16.0	2.650e+12	4.760e+08	1.540e+08	1.340e+09	1.030e+10
16.6	2.650e+12	5.330e+08	1.850e+08	1.510e+09	1.130e+10
17.2	2.650e+12	5.960e+08	2.210e+08	1.690e+09	1.250e+10
17.7	2.650e+12	6.650e+08	2.620e+08	1.880e+09	1.370e+10
18.3	2.650e+12	7.390e+08	3.100e+08	2.090e+09	1.500e+10
18.9	2.650e+12	8.210e+08	3.640e+08	2.320e+09	1.630e+10
19.4	2.650e+12	9.090e+08	4.260e+08	2.570e+09	1.780e+10

20.0	2.650e+12	1.000e+09	4.960e+08	2.840e+09	1.930e+10
20.6	2.650e+12	1.110e+09	5.760e+08	3.120e+09	2.100e+10
21.2	2.650e+12	1.220e+09	6.660e+08	3.430e+09	2.270e+10
21.7	2.650e+12	1.340e+09	7.660e+08	3.750e+09	2.450e+10
22.3	2.650e+12	1.460e+09	8.790e+08	4.100e+09	2.640e+10
22.9	2.650e+12	1.600e+09	1.000e+09	4.480e+09	2.840e+10
23.4	2.650e+12	1.750e+09	1.140e+09	4.870e+09	3.060e+10
24.0	2.650e+12	1.900e+09	1.300e+09	5.290e+09	3.280e+10
24.6	2.650e+12	2.070e+09	1.470e+09	5.740e+09	3.510e+10
25.2	2.650e+12	2.250e+09	1.660e+09	6.210e+09	3.750e+10
25.7	2.650e+12	2.440e+09	1.870e+09	6.710e+09	4.000e+10
26.3	2.650e+12	2.640e+09	2.100e+09	7.240e+09	4.270e+10
26.9	2.650e+12	2.860e+09	2.350e+09	7.800e+09	4.540e+10
27.4	2.650e+12	3.080e+09	2.630e+09	8.390e+09	4.830e+10
28.0	2.650e+12	3.330e+09	2.930e+09	9.010e+09	5.130e+10
28.6	2.650e+12	3.580e+09	3.250e+09	9.660e+09	5.440e+10
29.2	2.650e+12	3.850e+09	3.610e+09	1.030e+10	5.760e+10
29.7	2.650e+12	4.130e+09	4.000e+09	1.110e+10	6.090e+10
30.3	2.650e+12	4.430e+09	4.410e+09	1.180e+10	6.440e+10
30.9	2.650e+12	4.750e+09	4.870e+09	1.260e+10	6.790e+10
31.5	2.650e+12	5.080e+09	5.350e+09	1.340e+10	7.160e+10
32.0	2.650e+12	5.430e+09	5.880e+09	1.430e+10	7.540e+10
32.6	2.650e+12	5.800e+09	6.450e+09	1.520e+10	7.940e+10
33.2	2.650e+12	6.190e+09	7.050e+09	1.610e+10	8.340e+10
33.7	2.650e+12	6.590e+09	7.710e+09	1.710e+10	8.760e+10
34.3	2.650e+12	7.020e+09	8.400e+09	1.810e+10	9.190e+10
34.9	2.650e+12	7.460e+09	9.150e+09	1.920e+10	9.630e+10
35.5	2.650e+12	7.930e+09	9.950e+09	2.030e+10	1.010e+11
36.0	2.650e+12	8.410e+09	1.080e+10	2.140e+10	1.060e+11
36.6	2.650e+12	8.920e+09	1.170e+10	2.260e+10	1.100e+11
37.2	2.650e+12	9.450e+09	1.270e+10	2.380e+10	1.150e+11
37.7	2.650e+12	1.000e+10	1.370e+10	2.510e+10	1.200e+11
38.3	2.650e+12	1.060e+10	1.480e+10	2.640e+10	1.260e+11
38.9	2.650e+12	1.120e+10	1.590e+10	2.780e+10	1.310e+11
39.5	2.650e+12	1.180e+10	1.720e+10	2.920e+10	1.360e+11
40.0	2.650e+12	1.250e+10	1.850e+10	3.070e+10	1.420e+11
40.6	2.650e+12	1.310e+10	1.980e+10	3.220e+10	1.480e+11
41.2	2.650e+12	1.380e+10	2.130e+10	3.370e+10	1.540e+11
41.7	2.650e+12	1.460e+10	2.280e+10	3.540e+10	1.600e+11
42.3	2.650e+12	1.530e+10	2.440e+10	3.700e+10	1.660e+11
42.9	2.650e+12	1.610e+10	2.610e+10	3.870e+10	1.720e+11
43.5	2.650e+12	1.690e+10	2.790e+10	4.050e+10	1.790e+11
44.0	2.650e+12	1.770e+10	2.980e+10	4.230e+10	1.850e+11
44.6	2.650e+12	1.860e+10	3.170e+10	4.420e+10	1.920e+11
45.2	2.650e+12	1.950e+10	3.380e+10	4.610e+10	1.990e+11
45.7	2.650e+12	2.040e+10	3.600e+10	4.800e+10	2.050e+11
46.3	2.650e+12	2.140e+10	3.820e+10	5.010e+10	2.130e+11
46.9	2.650e+12	2.240e+10	4.060e+10	5.220e+10	2.200e+11
47.5	2.650e+12	2.340e+10	4.310e+10	5.430e+10	2.270e+11
48.0	2.650e+12	2.450e+10	4.570e+10	5.650e+10	2.350e+11
48.6	2.650e+12	2.560e+10	4.840e+10	5.870e+10	2.420e+11
49.2	2.650e+12	2.670e+10	5.130e+10	6.100e+10	2.500e+11
49.7	2.650e+12	2.790e+10	5.420e+10	6.340e+10	2.580e+11
50.3	2.650e+12	2.910e+10	5.730e+10	6.580e+10	2.660e+11
50.9	2.650e+12	3.030e+10	6.050e+10	6.830e+10	2.740e+11
51.5	2.650e+12	3.160e+10	6.390e+10	7.080e+10	2.820e+11
52.0	2.650e+12	3.290e+10	6.740e+10	7.340e+10	2.910e+11
52.6	2.650e+12	3.420e+10	7.100e+10	7.610e+10	2.990e+11
53.2	2.650e+12	3.560e+10	7.470e+10	7.880e+10	3.080e+11
53.8	2.650e+12	3.700e+10	7.870e+10	8.160e+10	3.160e+11
54.3	2.650e+12	3.850e+10	8.270e+10	8.440e+10	3.250e+11
54.9	2.650e+12	4.000e+10	8.690e+10	8.730e+10	3.340e+11
55.5	2.650e+12	4.150e+10	9.130e+10	9.020e+10	3.440e+11
56.0	2.650e+12	4.310e+10	9.580e+10	9.330e+10	3.530e+11
56.6	2.650e+12	4.470e+10	1.010e+11	9.630e+10	3.620e+11

57.2	2.650e+12	4.640e+10	1.050e+11	9.950e+10	3.720e+11
57.8	2.650e+12	4.810e+10	1.100e+11	1.030e+11	3.820e+11
58.3	2.650e+12	4.980e+10	1.160e+11	1.060e+11	3.910e+11
58.9	2.650e+12	5.160e+10	1.210e+11	1.090e+11	4.010e+11
59.5	2.650e+12	5.350e+10	1.270e+11	1.130e+11	4.110e+11
60.0	2.650e+12	5.530e+10	1.320e+11	1.160e+11	4.220e+11
60.6	2.650e+12	5.730e+10	1.380e+11	1.200e+11	4.320e+11
61.2	2.650e+12	5.920e+10	1.440e+11	1.230e+11	4.420e+11
61.8	2.650e+12	6.120e+10	1.510e+11	1.270e+11	4.530e+11
62.3	2.650e+12	6.330e+10	1.570e+11	1.300e+11	4.630e+11
62.9	2.650e+12	6.540e+10	1.640e+11	1.340e+11	4.740e+11
63.5	2.650e+12	6.760e+10	1.710e+11	1.380e+11	4.850e+11
64.0	2.650e+12	6.980e+10	1.780e+11	1.420e+11	4.960e+11
64.6	2.650e+12	7.200e+10	1.850e+11	1.460e+11	5.070e+11
65.2	2.650e+12	7.430e+10	1.930e+11	1.500e+11	5.190e+11
65.8	2.650e+12	7.660e+10	2.010e+11	1.540e+11	5.300e+11
66.3	2.650e+12	7.900e+10	2.090e+11	1.580e+11	5.420e+11
66.9	2.650e+12	8.150e+10	2.170e+11	1.620e+11	5.530e+11
67.5	2.650e+12	8.400e+10	2.250e+11	1.670e+11	5.650e+11
68.0	2.650e+12	8.650e+10	2.340e+11	1.710e+11	5.770e+11
68.6	2.650e+12	8.910e+10	2.430e+11	1.750e+11	5.890e+11
69.2	2.650e+12	9.170e+10	2.520e+11	1.800e+11	6.010e+11
69.8	2.650e+12	9.440e+10	2.620e+11	1.840e+11	6.130e+11
70.3	2.650e+12	9.720e+10	2.710e+11	1.890e+11	6.250e+11
70.9	2.650e+12	1.000e+11	2.810e+11	1.940e+11	6.380e+11
71.5	2.650e+12	1.030e+11	2.910e+11	1.980e+11	6.500e+11
72.1	2.650e+12	1.060e+11	3.020e+11	2.030e+11	6.630e+11
72.6	2.650e+12	1.090e+11	3.120e+11	2.080e+11	6.760e+11
73.2	2.650e+12	1.120e+11	3.230e+11	2.130e+11	6.890e+11
73.8	2.650e+12	1.150e+11	3.340e+11	2.180e+11	7.020e+11
74.3	2.650e+12	1.180e+11	3.460e+11	2.230e+11	7.150e+11
74.9	2.650e+12	1.210e+11	3.580e+11	2.280e+11	7.280e+11
75.5	2.650e+12	1.240e+11	3.700e+11	2.330e+11	7.410e+11
76.1	2.650e+12	1.280e+11	3.820e+11	2.380e+11	7.550e+11
76.6	2.650e+12	1.310e+11	3.950e+11	2.430e+11	7.680e+11
77.2	2.650e+12	1.340e+11	4.070e+11	2.490e+11	7.820e+11
77.8	2.650e+12	1.380e+11	4.210e+11	2.540e+11	7.960e+11
78.3	2.650e+12	1.410e+11	4.340e+11	2.600e+11	8.100e+11
78.9	2.650e+12	1.450e+11	4.480e+11	2.650e+11	8.230e+11
79.5	2.650e+12	1.480e+11	4.620e+11	2.710e+11	8.380e+11
80.1	2.650e+12	1.520e+11	4.760e+11	2.760e+11	8.520e+11
80.6	2.650e+12	1.560e+11	4.910e+11	2.820e+11	8.660e+11
81.2	2.650e+12	1.600e+11	5.050e+11	2.880e+11	8.800e+11
81.8	2.650e+12	1.640e+11	5.210e+11	2.940e+11	8.950e+11
82.3	2.650e+12	1.670e+11	5.360e+11	3.000e+11	9.090e+11
82.9	2.650e+12	1.710e+11	5.520e+11	3.060e+11	9.240e+11
83.5	2.650e+12	1.750e+11	5.680e+11	3.120e+11	9.390e+11
84.1	2.650e+12	1.800e+11	5.850e+11	3.180e+11	9.540e+11
84.6	2.650e+12	1.840e+11	6.020e+11	3.240e+11	9.690e+11
85.2	2.650e+12	1.880e+11	6.190e+11	3.300e+11	9.840e+11
85.8	2.650e+12	1.920e+11	6.360e+11	3.360e+11	9.990e+11
86.3	2.650e+12	1.960e+11	6.540e+11	3.430e+11	1.010e+12
86.9	2.650e+12	2.010e+11	6.720e+11	3.490e+11	1.030e+12
87.5	2.650e+12	2.050e+11	6.900e+11	3.550e+11	1.040e+12
88.1	2.650e+12	2.100e+11	7.090e+11	3.620e+11	1.060e+12
88.6	2.650e+12	2.140e+11	7.280e+11	3.680e+11	1.080e+12
89.2	2.650e+12	2.190e+11	7.480e+11	3.750e+11	1.090e+12
89.8	2.650e+12	2.240e+11	7.680e+11	3.820e+11	1.110e+12
90.3	2.650e+12	2.290e+11	7.880e+11	3.880e+11	1.120e+12
90.9	2.650e+12	2.330e+11	8.080e+11	3.950e+11	1.140e+12
91.5	2.650e+12	2.380e+11	8.290e+11	4.020e+11	1.160e+12
92.1	2.650e+12	2.430e+11	8.500e+11	4.090e+11	1.170e+12
92.6	2.650e+12	2.480e+11	8.720e+11	4.160e+11	1.190e+12
93.2	2.650e+12	2.530e+11	8.940e+11	4.230e+11	1.200e+12
93.8	2.650e+12	2.580e+11	9.160e+11	4.300e+11	1.220e+12

94.4	2.650e+12	2.640e+11	9.390e+11	4.370e+11	1.240e+12
94.9	2.650e+12	2.690e+11	9.620e+11	4.440e+11	1.250e+12
95.5	2.650e+12	2.740e+11	9.850e+11	4.510e+11	1.270e+12
96.1	2.650e+12	2.800e+11	1.010e+12	4.590e+11	1.290e+12
96.6	2.650e+12	2.850e+11	1.030e+12	4.660e+11	1.300e+12
97.2	2.650e+12	2.910e+11	1.060e+12	4.730e+11	1.320e+12
97.8	2.650e+12	2.960e+11	1.080e+12	4.810e+11	1.340e+12
98.4	2.650e+12	3.020e+11	1.110e+12	4.880e+11	1.350e+12
98.9	2.650e+12	3.070e+11	1.130e+12	4.960e+11	1.370e+12
99.5	2.650e+12	3.130e+11	1.160e+12	5.030e+11	1.390e+12
100.1	2.650e+12	3.190e+11	1.190e+12	5.110e+11	1.410e+12
100.6	2.650e+12	3.250e+11	1.210e+12	5.190e+11	1.420e+12
101.2	2.650e+12	3.310e+11	1.240e+12	5.270e+11	1.440e+12
101.8	2.650e+12	3.370e+11	1.270e+12	5.340e+11	1.460e+12
102.4	2.650e+12	3.430e+11	1.300e+12	5.420e+11	1.480e+12
102.9	2.650e+12	3.490e+11	1.320e+12	5.500e+11	1.490e+12
103.5	2.650e+12	3.560e+11	1.350e+12	5.580e+11	1.510e+12
104.1	2.650e+12	3.620e+11	1.380e+12	5.660e+11	1.530e+12
104.6	2.650e+12	3.680e+11	1.410e+12	5.740e+11	1.550e+12
105.2	2.650e+12	3.750e+11	1.440e+12	5.820e+11	1.570e+12
105.8	2.650e+12	3.810e+11	1.470e+12	5.910e+11	1.580e+12
106.4	2.650e+12	3.880e+11	1.500e+12	5.990e+11	1.600e+12
106.9	2.650e+12	3.940e+11	1.530e+12	6.070e+11	1.620e+12
107.5	2.650e+12	4.010e+11	1.570e+12	6.150e+11	1.640e+12
108.1	2.650e+12	4.080e+11	1.600e+12	6.240e+11	1.660e+12
108.6	2.650e+12	4.150e+11	1.630e+12	6.320e+11	1.680e+12
109.2	2.650e+12	4.210e+11	1.660e+12	6.410e+11	1.690e+12
109.8	2.650e+12	4.280e+11	1.700e+12	6.490e+11	1.710e+12
110.4	2.650e+12	4.350e+11	1.730e+12	6.580e+11	1.730e+12
110.9	2.650e+12	4.430e+11	1.760e+12	6.660e+11	1.750e+12
111.5	2.650e+12	4.500e+11	1.800e+12	6.750e+11	1.770e+12
112.1	2.650e+12	4.570e+11	1.830e+12	6.840e+11	1.790e+12
112.7	2.650e+12	4.640e+11	1.870e+12	6.920e+11	1.810e+12
113.2	2.650e+12	4.720e+11	1.900e+12	7.010e+11	1.830e+12
113.8	2.650e+12	4.790e+11	1.940e+12	7.100e+11	1.840e+12
114.4	2.650e+12	4.870e+11	1.980e+12	7.190e+11	1.860e+12
114.9	2.650e+12	4.940e+11	2.010e+12	7.280e+11	1.880e+12
115.5	2.650e+12	5.020e+11	2.050e+12	7.370e+11	1.900e+12
116.1	2.650e+12	5.090e+11	2.090e+12	7.460e+11	1.920e+12
116.7	2.650e+12	5.170e+11	2.130e+12	7.550e+11	1.940e+12
117.2	2.650e+12	5.250e+11	2.170e+12	7.640e+11	1.960e+12
117.8	2.650e+12	5.330e+11	2.210e+12	7.730e+11	1.980e+12
118.4	2.650e+12	5.410e+11	2.250e+12	7.820e+11	2.000e+12
118.9	2.650e+12	5.490e+11	2.290e+12	7.910e+11	2.020e+12
119.5	2.650e+12	5.570e+11	2.330e+12	8.010e+11	2.040e+12
120.1	2.650e+12	5.650e+11	2.370e+12	8.100e+11	2.060e+12
120.7	2.650e+12	5.730e+11	2.410e+12	8.190e+11	2.080e+12
121.2	2.650e+12	5.820e+11	2.450e+12	8.290e+11	2.100e+12
121.8	2.650e+12	5.900e+11	2.490e+12	8.380e+11	2.120e+12
122.4	2.650e+12	5.980e+11	2.540e+12	8.480e+11	2.140e+12
122.9	2.650e+12	6.070e+11	2.580e+12	8.570e+11	2.160e+12
123.5	2.650e+12	6.150e+11	2.620e+12	8.670e+11	2.180e+12
124.1	2.650e+12	6.240e+11	2.670e+12	8.760e+11	2.200e+12
124.7	2.650e+12	6.330e+11	2.710e+12	8.860e+11	2.220e+12
125.2	2.650e+12	6.420e+11	2.760e+12	8.960e+11	2.240e+12
125.8	2.650e+12	6.500e+11	2.800e+12	9.050e+11	2.260e+12
126.4	2.650e+12	6.590e+11	2.850e+12	9.150e+11	2.280e+12
126.9	2.650e+12	6.680e+11	2.890e+12	9.250e+11	2.300e+12
127.5	2.650e+12	6.770e+11	2.940e+12	9.350e+11	2.320e+12
128.1	2.650e+12	6.860e+11	2.990e+12	9.450e+11	2.340e+12
128.7	2.650e+12	6.960e+11	3.030e+12	9.550e+11	2.360e+12
129.2	2.650e+12	7.050e+11	3.080e+12	9.650e+11	2.380e+12
129.8	2.650e+12	7.140e+11	3.130e+12	9.750e+11	2.400e+12
130.4	2.650e+12	7.240e+11	3.180e+12	9.850e+11	2.430e+12
130.9	2.650e+12	7.330e+11	3.230e+12	9.950e+11	2.450e+12

131.5	2.650e+12	7.420e+11	3.280e+12	1.000e+12	2.470e+12
132.1	2.650e+12	7.520e+11	3.330e+12	1.010e+12	2.490e+12
132.7	2.650e+12	7.620e+11	3.380e+12	1.030e+12	2.510e+12
133.2	2.650e+12	7.710e+11	3.430e+12	1.040e+12	2.530e+12
133.8	2.650e+12	7.810e+11	3.480e+12	1.050e+12	2.550e+12
134.4	2.650e+12	7.910e+11	3.540e+12	1.060e+12	2.570e+12
135.0	2.650e+12	8.010e+11	3.590e+12	1.070e+12	2.590e+12
135.5	2.650e+12	8.110e+11	3.640e+12	1.080e+12	2.620e+12
136.1	2.650e+12	8.210e+11	3.700e+12	1.090e+12	2.640e+12
136.7	2.650e+12	8.310e+11	3.750e+12	1.100e+12	2.660e+12

A.6 Supplemental Plots for the Acetyl + Oxygen System and its Perturbations

Normal (Unperturbed) System

Supplemental plots for the normal acetyl + oxygen system (i.e. using the potential energy surface as shown in Figure 3) are given in Figures 12 and 13. These plots show the $k(T,P)$ values for reactions that involve one of the two isomers (acetylperoxy or hydroperoxylvinoxy) as the reactant. These $k(T,P)$ values can be important under certain conditions even when starting from acetyl + oxygen; furthermore, in other systems you might be interested in starting from an isomer configuration rather than a set of reactants. Thus, it is also important to obtain reasonably accurate estimates of these phenomenological rate coefficients.

As with the $k(T,P)$ values for acetyl + oxygen as the reactant (see Figure 5 in the text), there are primarily two regions of disagreement between the three methods:

- At low pressure, the modified strong collision (MSC) method predicts a slower rate of falloff for $\mathrm{CH_3CO + O_2 \rightleftharpoons CH_3C(O)OO}$ and $\mathrm{CH_3CO + O_2 \rightleftharpoons CH_2C(O)OOH}$ than the other methods.

- At high temperature, the methods disagree significantly on the sharpness of the falloff (or even if one is present). In particular, the reservoir state (RS) method generally predicts a sharper falloff, the MSC method a shallower falloff, and the chemically-significant eigenvalues (CSE) method falls somewhere in between.

Note that these are the limits in which pressure dependence is very important, so it is unsurprising to see that the methods disagree significantly under these conditions. Unfortunately, we cannot ascertain which of the low-pressure and high-temperature behavior is correct just from this plot; for this we must look at concentration profiles (see Figure 6 in the text). When we do, we see that the RS and CSE methods have the correct behavior for the low-pressure disagreement, while the CSE is generally the most accurate for the high-temperature disagreement.

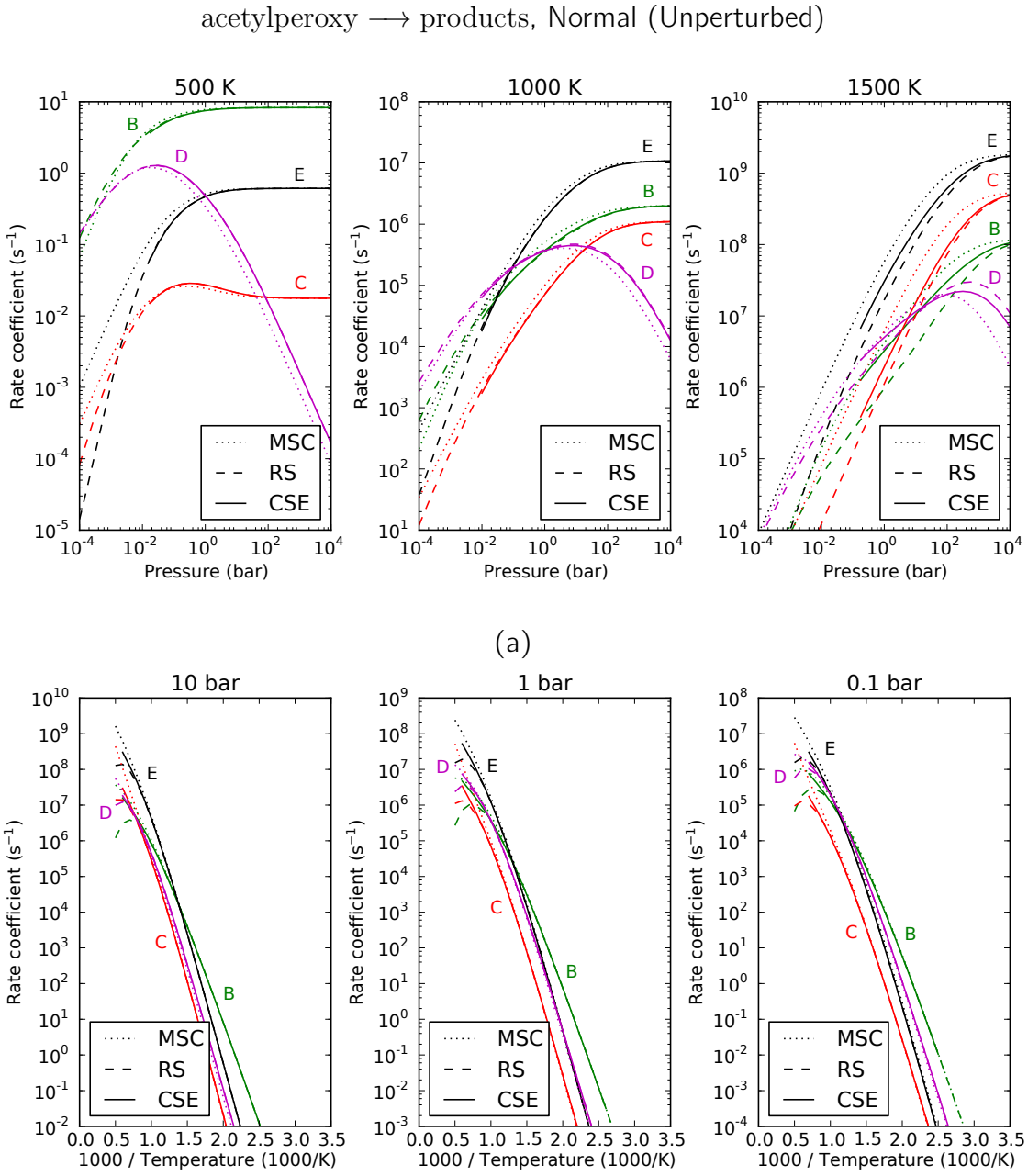

Figure 12: Comparison of rate coefficients versus (a) pressure and (b) temperature for $CH_3C(O)OO \rightarrow$ products estimated using the modified strong collision (MSC), reservoir state (RS), and chemically-significant eigenvalue (CSE) methods for the normal acetyl + oxygen system. In the plots, B = hydroperoxylvinoxy, C = ketene + HO_2, D = lactone + OH, and E = acetyl + O_2.

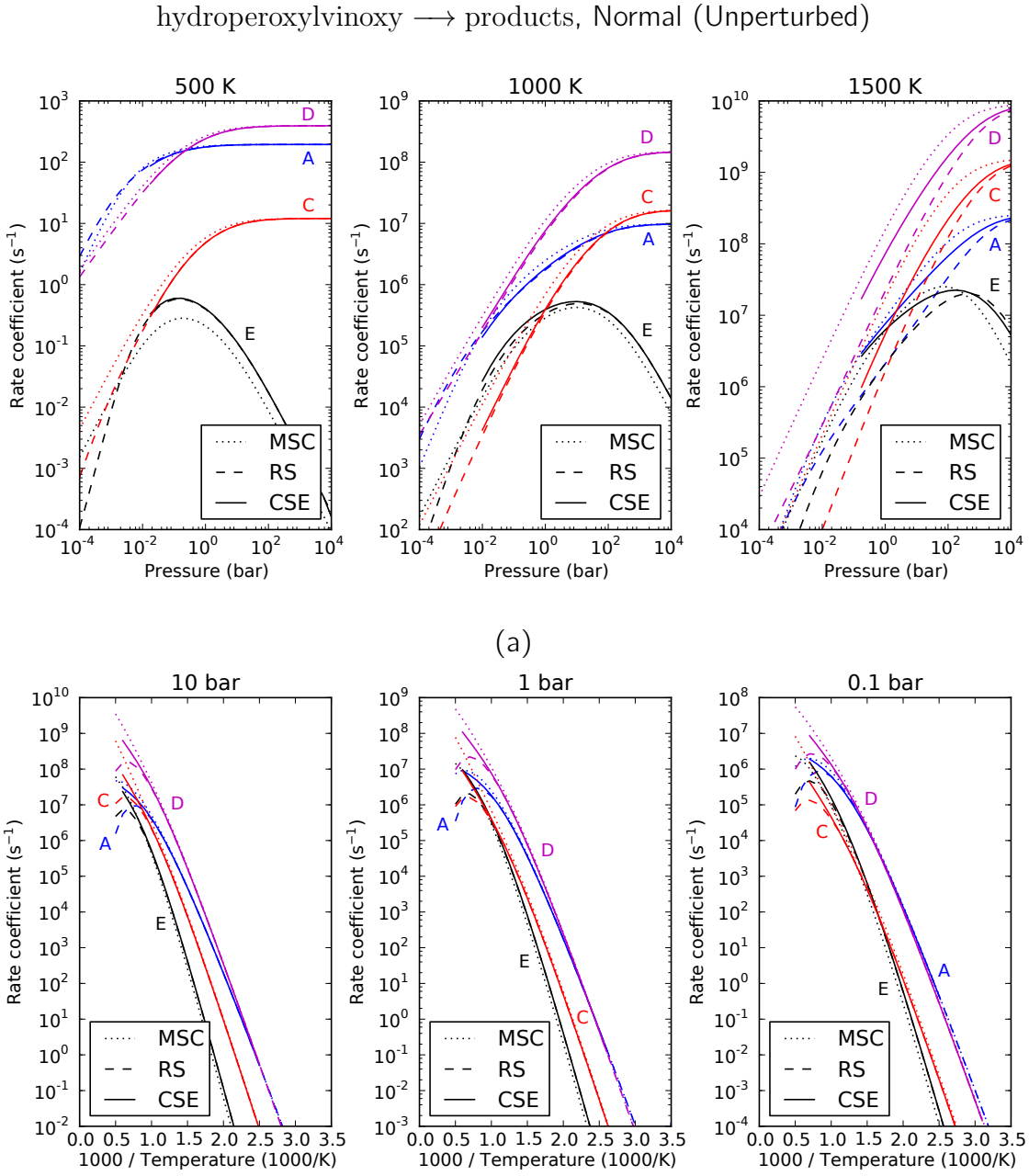

Figure 13: Comparison of rate coefficients versus (a) pressure and (b) temperature for $CH_2C(O)OOH \rightarrow$ products estimated using the modified strong collision (MSC), reservoir state (RS), and chemically-significant eigenvalue (CSE) methods for the normal acetyl + oxygen system. In the plots, A = acetylperoxy, C = ketene + HO_2, D = lactone + OH, and E = acetyl + O_2.

Perturbation 1: Acetyl + 20 kcal/mol

Supplemental plots for the acetyl + oxygen system with the acetyl + oxygen ground-state energy increased by 20 kcal/mol are given in Figures 14 to 17. This perturbation makes the low-pressure disagreement between the MSC method and the other methods much more exaggerated. The concentration profile comparsion confirms that the MSC method is significantly less accurate than the RS and CSE methods at low pressures, particularly for the initial adduct acetylperoxy. The high-temperature disagreement is not much different than in the normal acetyl + oxygen system.

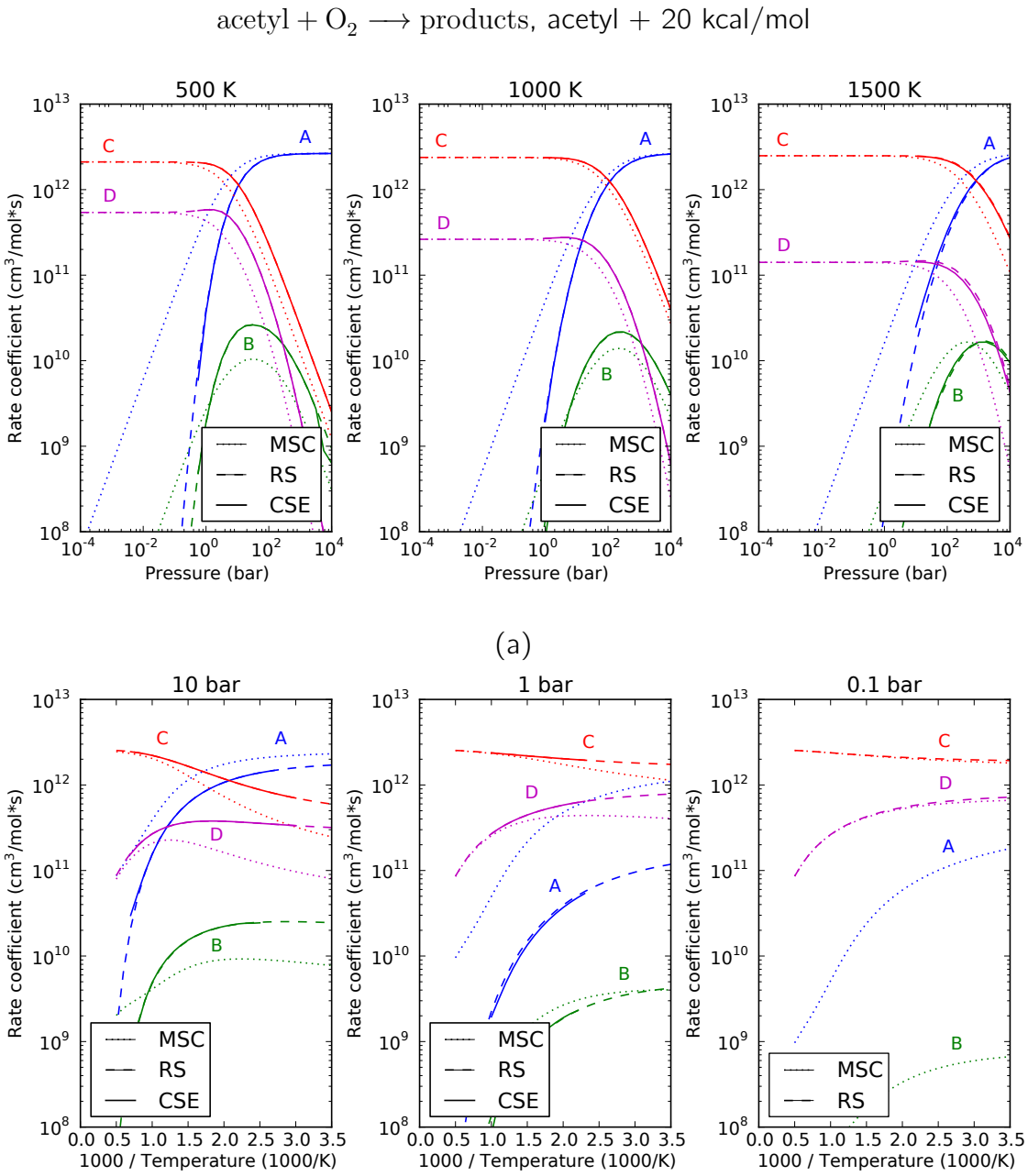

Figure 14: Comparison of rate coefficients versus (a) pressure and (b) temperature for $CH_3CO + O2 \rightarrow$ products estimated using the modified strong collision (MSC), reservoir state (RS), and chemically-significant eigenvalue (CSE) methods for the acetyl + oxygen system with the acetyl ground-state energy artifically increased by 20 kcal/mol. In the plots, A = acetylperoxy, B = hydroperoxylvinoxy, C = ketene + HO_2, and D = lactone + OH.

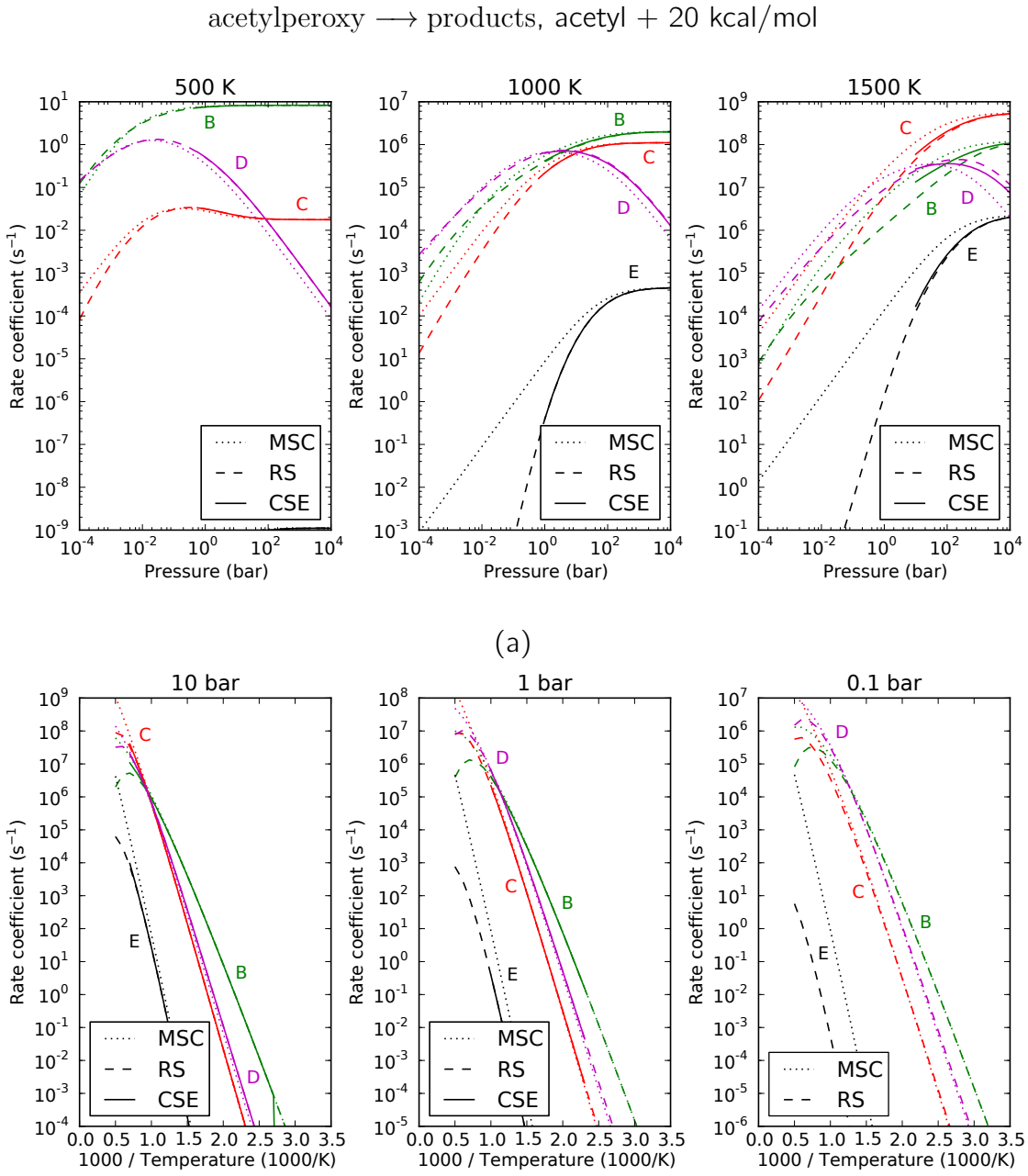

Figure 15: Comparison of rate coefficients versus (a) pressure and (b) temperature for $CH_3C(O)OO \rightarrow$ products estimated using the modified strong collision (MSC), reservoir state (RS), and chemically-significant eigenvalue (CSE) methods for the acetyl + oxygen system with the acetyl ground-state energy artifically increased by 20 kcal/mol. In the plots, B = hydroperoxylvinoxy, C = ketene + HO_2, D = lactone + OH, and E = acetyl + O_2.

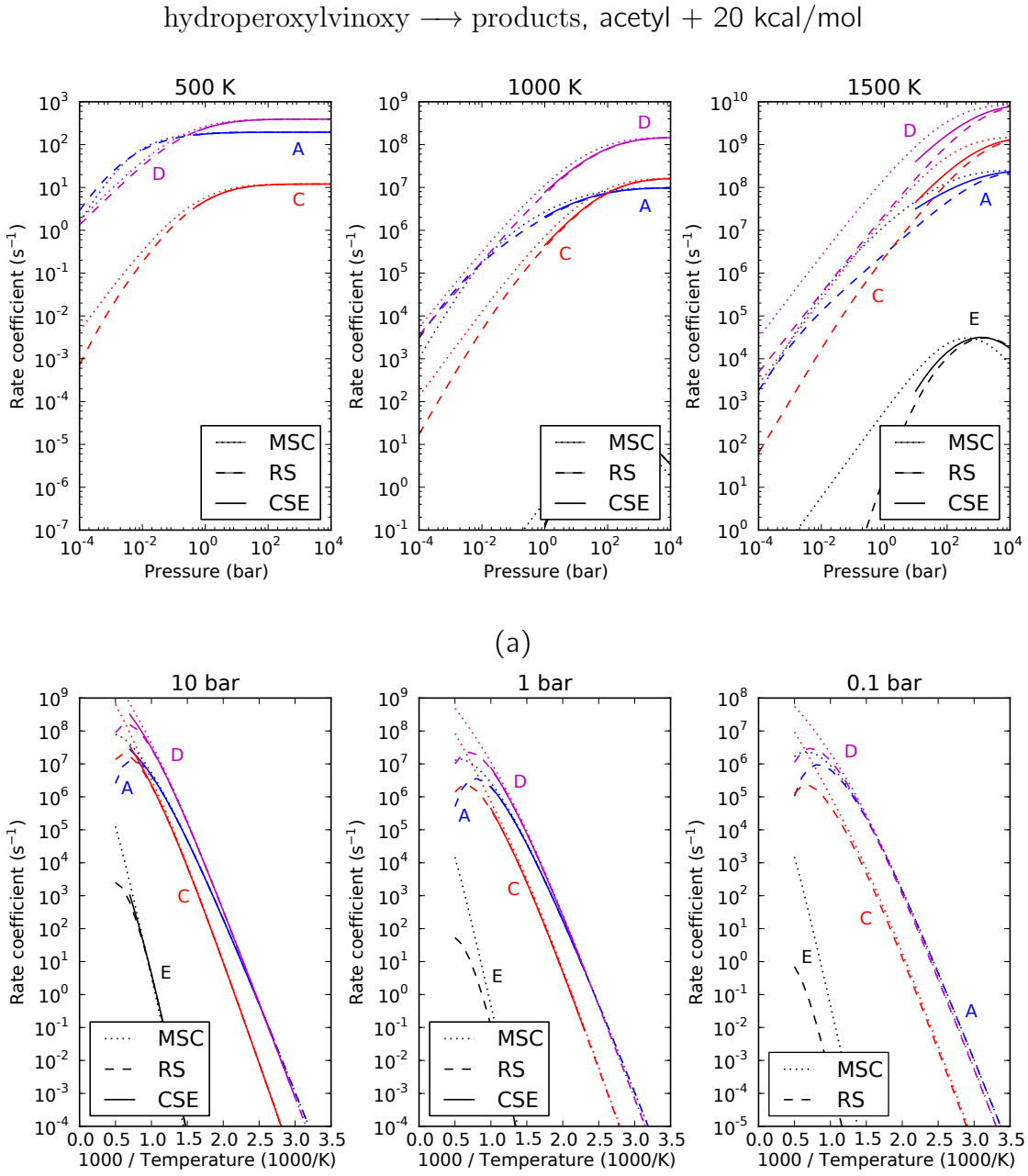

Figure 16: Comparison of rate coefficients versus (a) pressure and (b) temperature for $CH_2C(O)OOH \rightarrow$ products estimated using the modified strong collision (MSC), reservoir state (RS), and chemically-significant eigenvalue (CSE) methods for the acetyl + oxygen system with the acetyl ground-state energy artifically increased by 20 kcal/mol. In the plots, A = acetylperoxy, C = ketene + HO_2, D = lactone + OH, and E = acetyl + O_2.

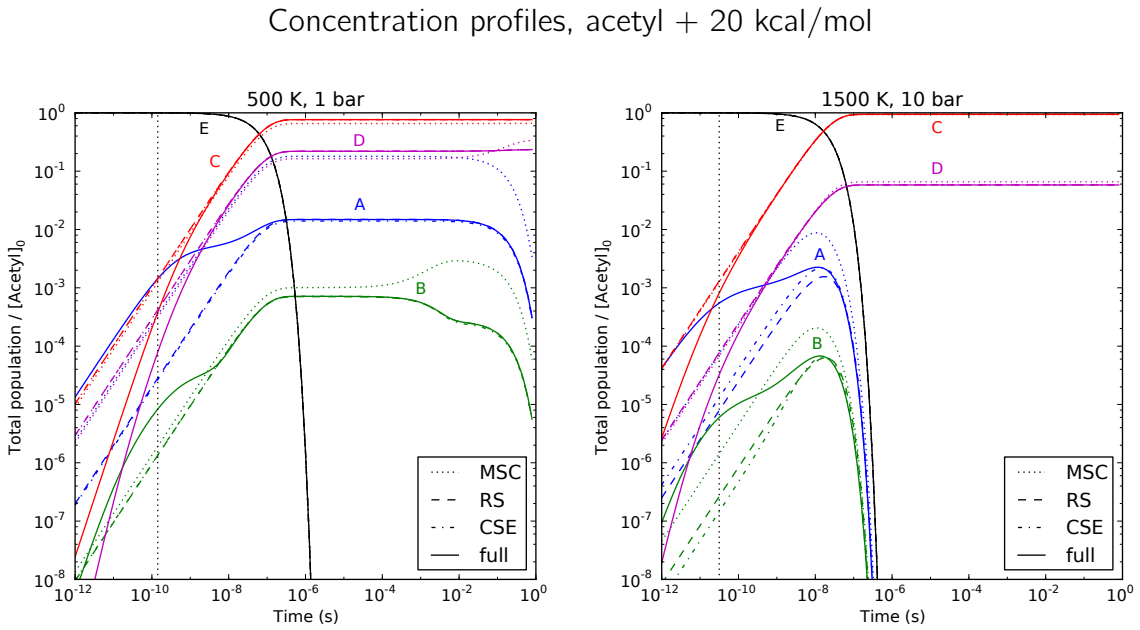

Figure 17: Concentration profiles at low-temperature and high-temperature conditions, comparing the modified strong collision (MSC), reservoir state (RS), and chemically-significant eigenvalue (CSE) methods with the full master equation solution for the acetyl + oxygen system with the acetyl ground-state energy artifically increased by 20 kcal/mol. In the plots, A = acetylperoxy, B = hydroperoxylvinoxy, C = ketene + HO_2, D = lactone + OH, and E = acetyl + O_2.

Perturbation 2: Acetylperoxy + 20 kcal/mol

Supplemental plots for the acetyl + oxygen system with the acetylperoxy ground-state energy increased by 20 kcal/mol are given in Figures 18 to 21. This perturbation also makes the low-pressure disagreement between the MSC method and the other methods more exaggerated, but only for $\mathrm{CH_3CO + O_2 \rightleftharpoons CH_3C(O)OO}$. There is now also significant disagreement between the RS and CSE methods at low pressures, especially very near the limit where the CSE curve ends (i.e. where a chemical eigenvalue merges into the internal energy eigenspectrum). Looking at the concentration profiles at 500 K and 10 bar, we see that the CSE method is the most accurate, with the MSC method overpredicting the rate (i.e. underpredicting the falloff) and the RS method underpredicting the rate. Thus, as stated in the text, we have a clear example of a case where the CSE method is more accurate than the others. Note that the $k(T, P)$ values for reactions involving acetylperoxy (the perturbed isomer) are most affected, often with drastic disagreement as pressure is lowered.

This perturbation also exaggerates the high-temperature disagreement. Unfortunately, the CSE method cannot resolve three chemical eigenvalues at the conditions of disagreement, so we can only compare the MSC and RS methods to the full solution. Doing this at 1500 K and 10 bar suggests that the sharper falloff predicted by the RS method is not very accurate, while the more gentle falloff predicted by the MSC method is closer to the truth. At high temperatures the majority of the Boltzmann population of acetylperoxy exists in reactive energy grains, especially in the perturbed system. This indicates that the reservoir state approximation is invalid, so it is not surprising to see the RS method give poor predictions. The single-step collision model used by the MSC method may actually be a reasonable approximation for shallow wells, particularly when including the collision efficiency $\beta(T)$.

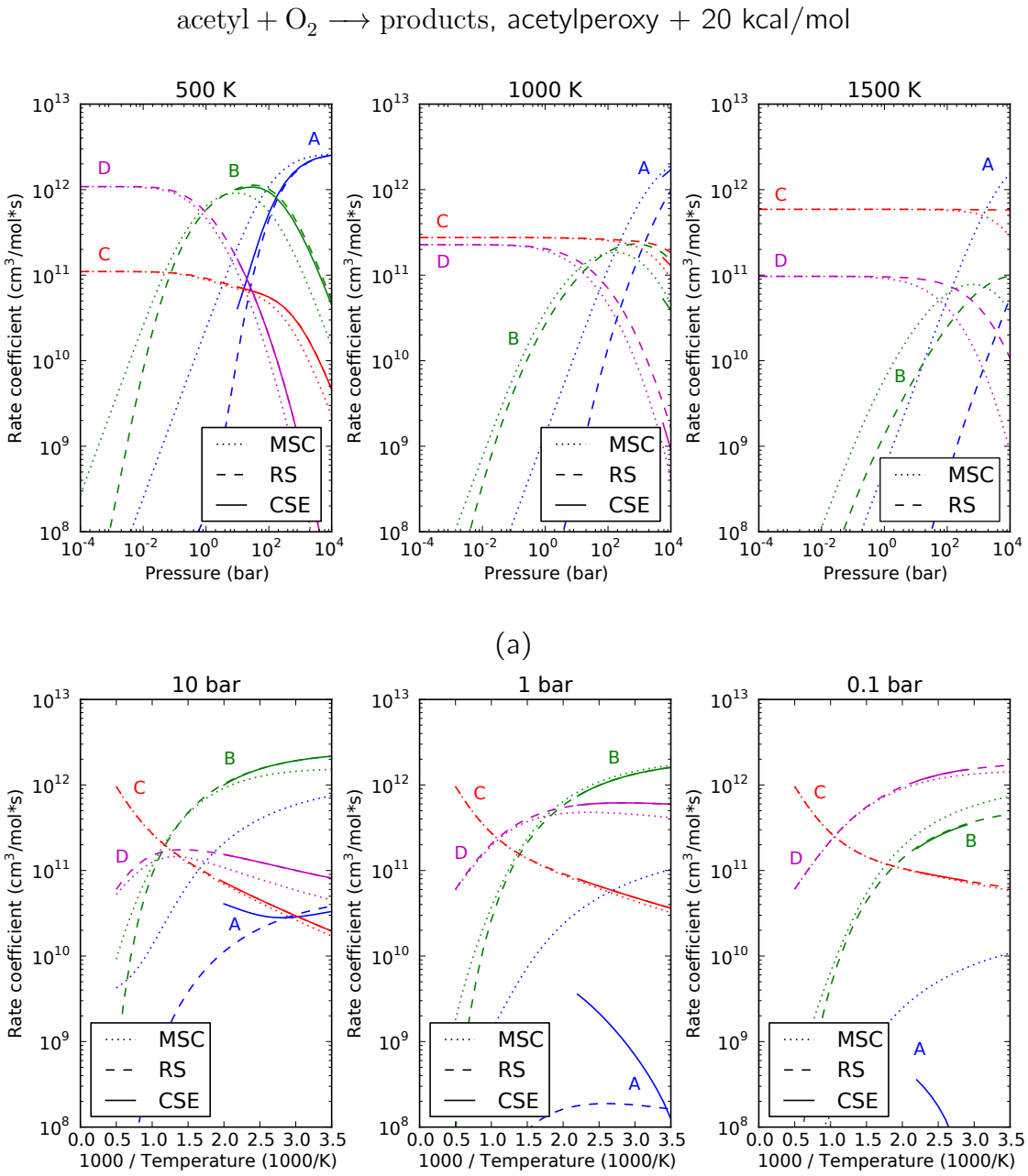

Figure 18: Comparison of rate coefficients versus (a) pressure and (b) temperature for $CH_3CO + O_2 \rightarrow$ products estimated using the modified strong collision (MSC), reservoir state (RS), and chemically-significant eigenvalue (CSE) methods for the acetyl + oxygen system with the acetylperoxy ground-state energy artifically increased by 20 kcal/mol. In the plots, A = acetylperoxy, B = hydroperoxylvinoxy, C = ketene + HO_2, and D = lactone + OH.

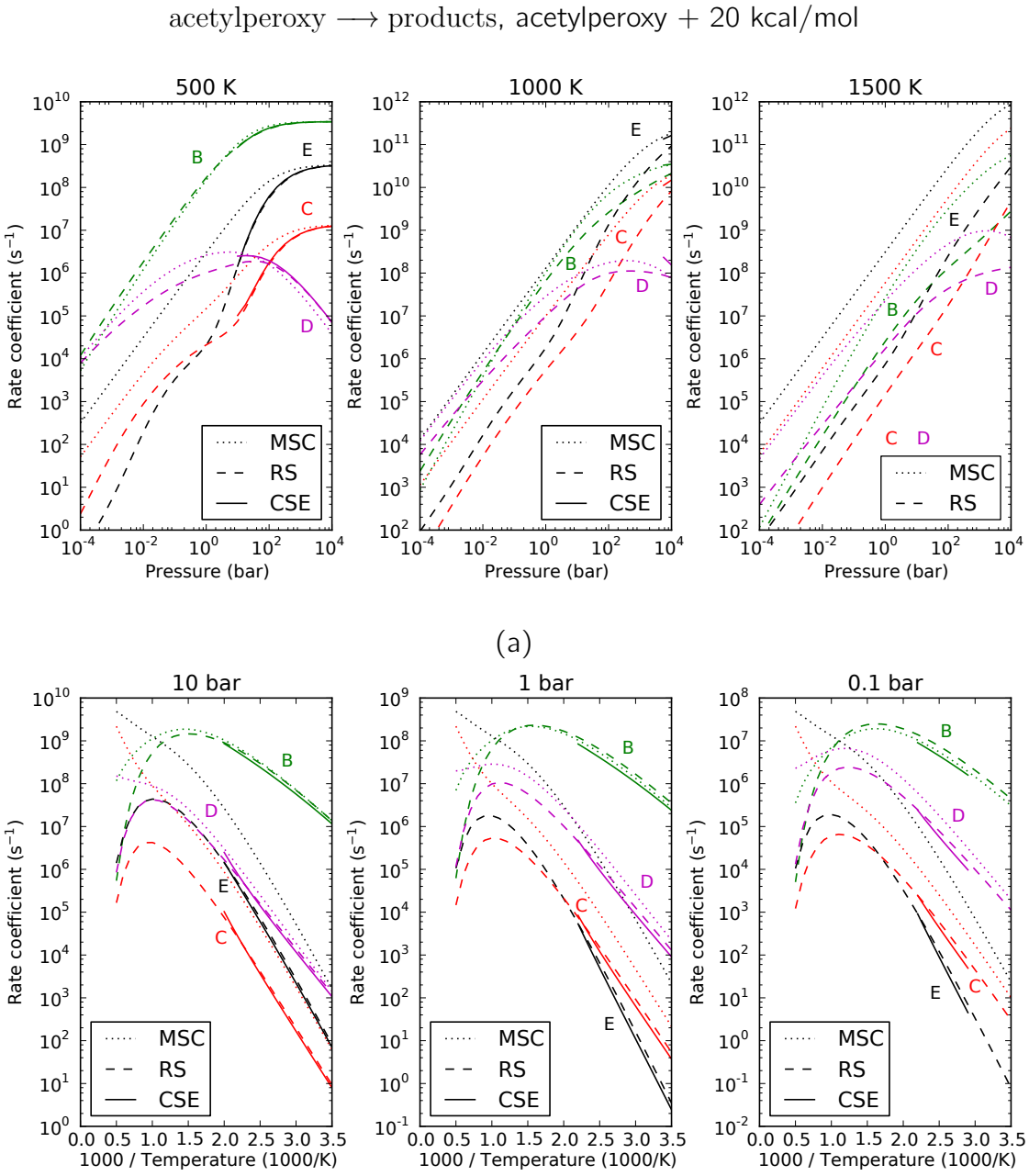

Figure 19: Comparison of rate coefficients versus (a) pressure and (b) temperature for $CH_3C(O)OO \rightarrow$ products estimated using the modified strong collision (MSC), reservoir state (RS), and chemically-significant eigenvalue (CSE) methods for the acetyl + oxygen system with the acetylperoxy ground-state energy artifically increased by 20 kcal/mol. In the plots, B = hydroperoxylvinoxy, C = ketene + HO_2, D = lactone + OH, and E = acetyl + O_2.

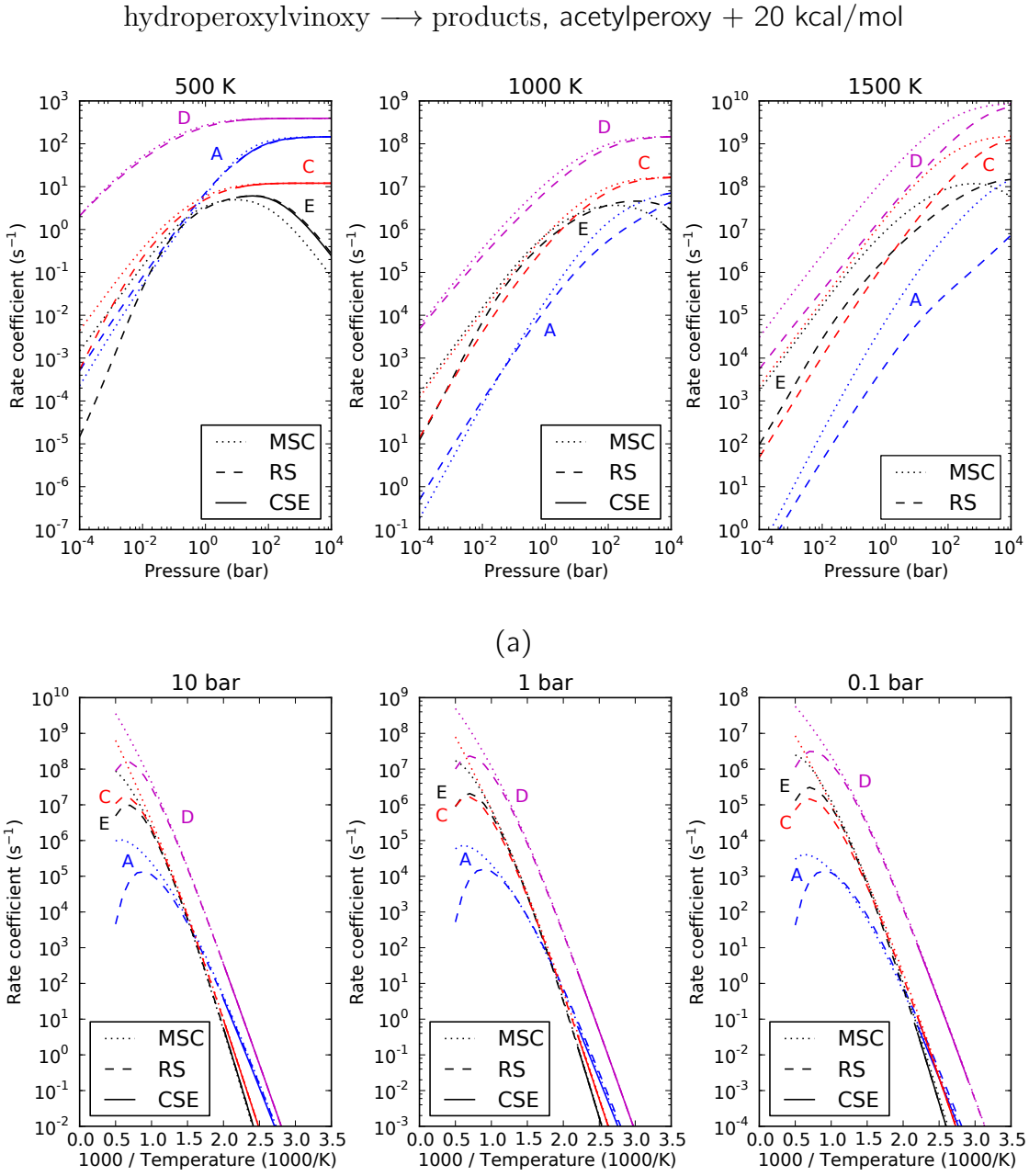

Figure 20: Comparison of rate coefficients versus (a) pressure and (b) temperature for $CH_2C(O)OOH \rightarrow$ products estimated using the modified strong collision (MSC), reservoir state (RS), and chemically-significant eigenvalue (CSE) methods for the acetyl + oxygen system with the acetylperoxy ground-state energy artifically increased by 20 kcal/mol. In the plots, A = acetylperoxy, C = ketene + HO_2, D = lactone + OH, and E = acetyl + O_2.

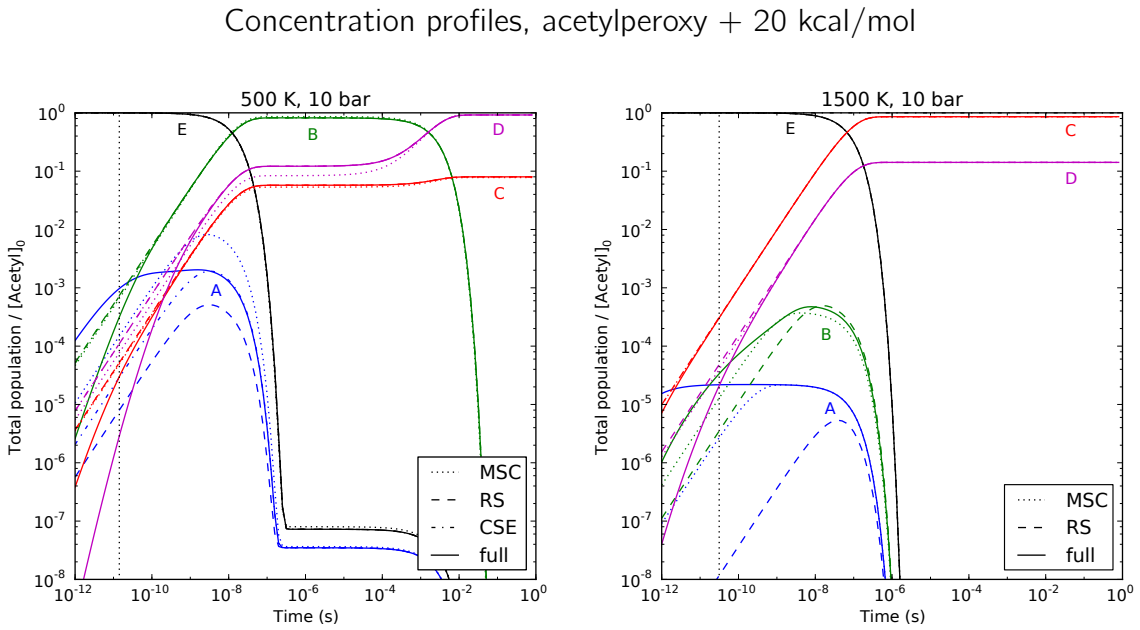

Figure 21: Concentration profiles at low-temperature and high-temperature conditions, comparing the modified strong collision (MSC), reservoir state (RS), and chemically-significant eigenvalue (CSE) methods with the full master equation solution for the acetyl + oxygen system with the acetylperoxy ground-state energy artifically increased by 20 kcal/mol. In the plots, A = acetylperoxy, B = hydroperoxylvinoxy, C = ketene + HO_2, D = lactone + OH, and E = acetyl + O_2.

Perturbation 3: Hydroperoxylvinoxy + 20 kcal/mol

Supplemental plots for the acetyl + oxygen system with the acetylperoxy ground-state energy increased by 20 kcal/mol are given in Figures 22 to 25. This perturbation slows the $\mathrm{CH_3CO + O_2 \rightleftharpoons CH_2C(O)OOH}$ rate so much that it falls below the $k(T, P)$ range shown in Figure 22. The remaining $k(T, P)$ values show the same regions of agreement and disagreement as for the other perturbations. Notably, the pressure at which a chemical eigenvalue merges into the internal energy eigenspectrum for a given temperature is quite high for this perturbation, so the CSE method is almost completely cut off from the plots. As before, the $k(T, P)$ values for reactions involving the perturbed isomer hydroperoxylvinoxy are significantly affected, with the RS method underpredicting all of these rates at high temperature, while the MSC method performs better.

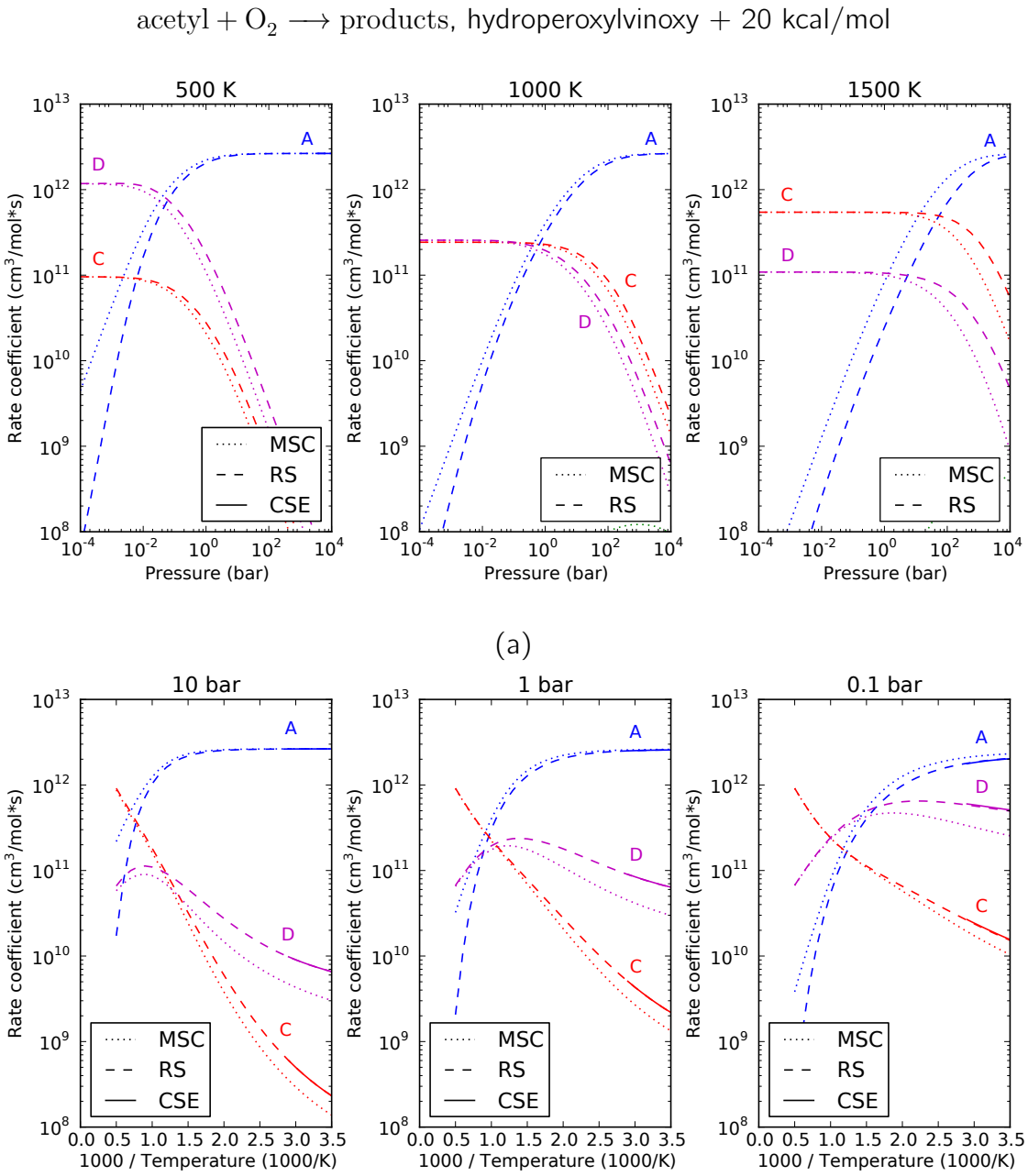

Figure 22: Comparison of rate coefficients versus (a) pressure and (b) temperature for $CH_3CO + O_2 \rightarrow$ products estimated using the modified strong collision (MSC), reservoir state (RS), and chemically-significant eigenvalue (CSE) methods for the acetyl + oxygen system with the hydroperoxylvinoxy ground-state energy artifically increased by 20 kcal/mol. In the plots, A = acetylperoxy, B = hydroperoxylvinoxy, C = ketene + HO_2, and D = lactone + OH.

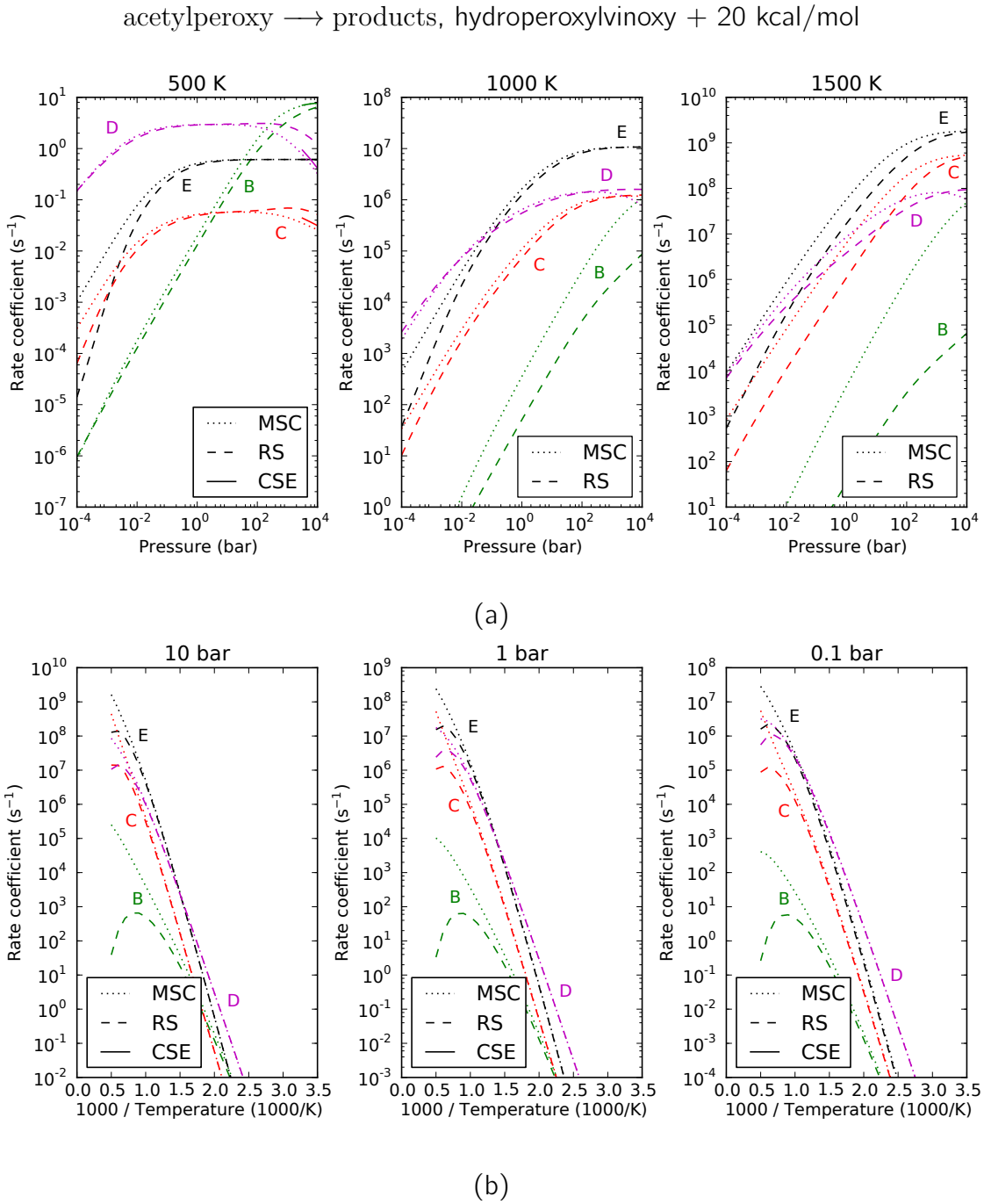

Figure 23: Comparison of rate coefficients versus (a) pressure and (b) temperature for $CH_3C(O)OO \rightarrow$ products estimated using the modified strong collision (MSC), reservoir state (RS), and chemically-significant eigenvalue (CSE) methods for the acetyl + oxygen system with the hydroperoxylvinoxy ground-state energy artifically increased by 20 kcal/mol. In the plots, B = hydroperoxylvinoxy, C = ketene + HO_2, D = lactone + OH, and E = acetyl + O_2.

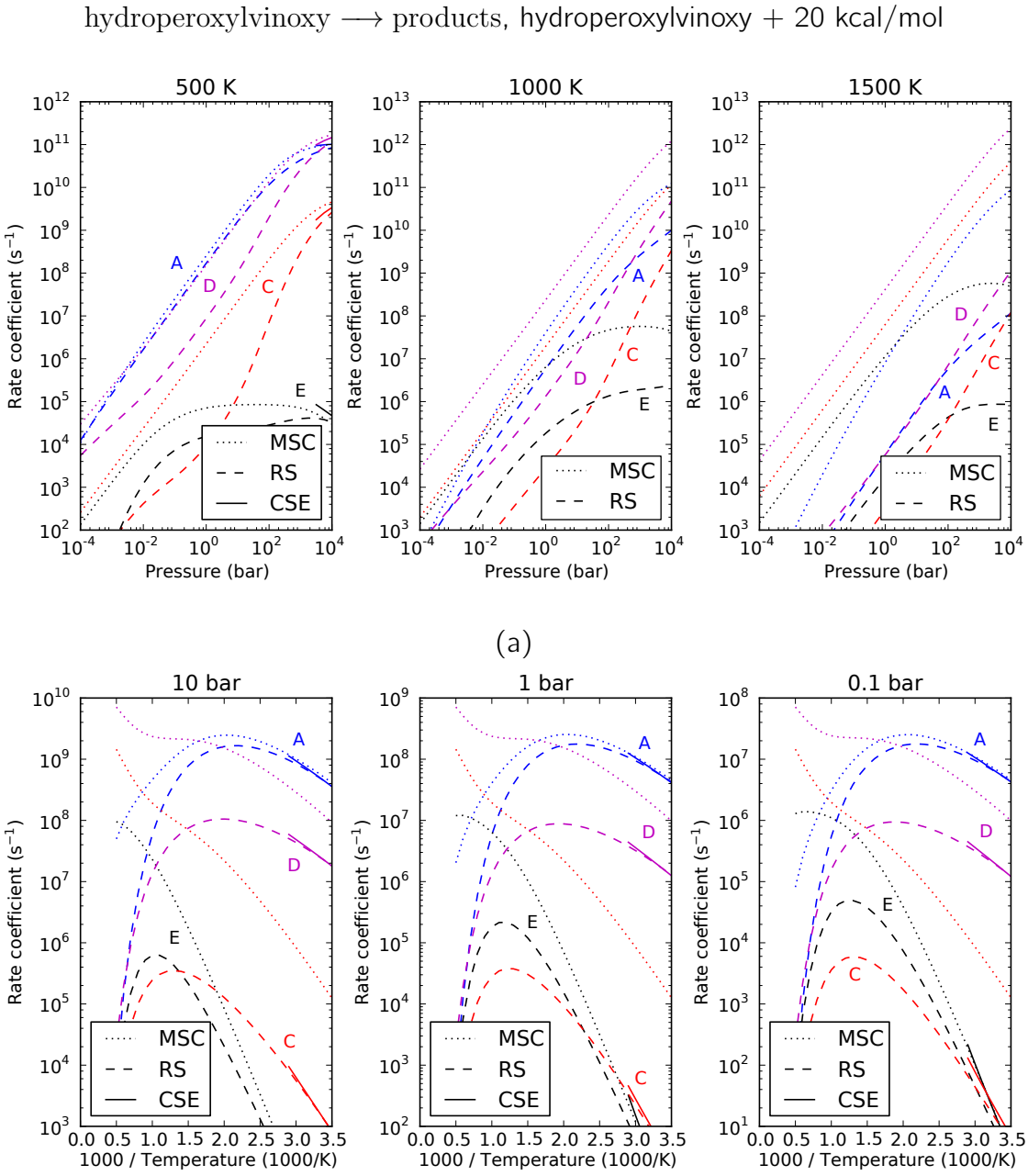

Figure 24: Comparison of rate coefficients versus (a) pressure and (b) temperature for $CH_2C(O)OOH \rightarrow$ products estimated using the modified strong collision (MSC), reservoir state (RS), and chemically-significant eigenvalue (CSE) methods for the acetyl + oxygen system with the hydroperoxylvinoxy ground-state energy artifically increased by 20 kcal/mol. In the plots, A = acetylperoxy, C = ketene + HO_2, D = lactone + OH, and E = acetyl + O_2.

Concentration profiles, hydroperoxylvinoxy + 20 kcal/mol

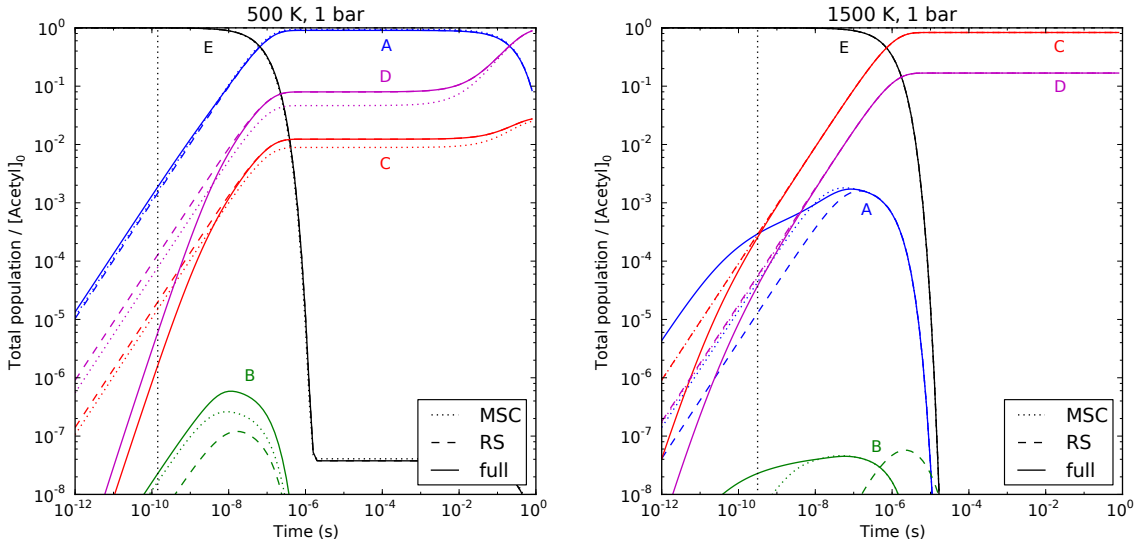

Figure 25: Concentration profiles at low-temperature and high-temperature conditions, comparing the modified strong collision (MSC), reservoir state (RS), and chemically-significant eigenvalue (CSE) methods with the full master equation solution for the acetyl + oxygen system with the hydroperoxylvinoxy ground-state energy artifically increased by 20 kcal/mol. In the plots, A = acetylperoxy, B = hydroperoxylvinoxy, C = ketene + HO_2, D = lactone + OH, and E = acetyl + O_2.

Perturbation 4: Isomerization - 20 kcal/mol

Supplemental plots for the acetyl + oxygen system with the acetylperoxy ground-state energy increased by 20 kcal/mol are given in Figures 26 to 29. This perturbation focuses on a single reaction $\mathrm{CH_3C(O)OO} \rightleftharpoons \mathrm{CH_2C(O)OOH}$, lowering the barrier in order to make this reaction very fast. Accordingly, the $k(T, P)$ values for $\mathrm{CH_3C(O)OO} \longrightarrow \mathrm{products}$ and $\mathrm{CH_2C(O)OOH} \longrightarrow \mathrm{products}$ indicate that this reaction is by far the fastest, except at high temperature. The high-temperature disagreement between the MSC and RS methods (as the CSE method is unable to resolve three chemical eigenvalues at the relevant conditions) is the most pronounced as we have seen in the perturbations considered. As before, concentration profile comparisons suggest the sharp falloff in the $\mathrm{CH_3C(O)OO} \rightleftharpoons \mathrm{CH_2C(O)OOH}$ rate predicted by the RS method is less accurate than the more gentle falloff predicted by the MSC method.

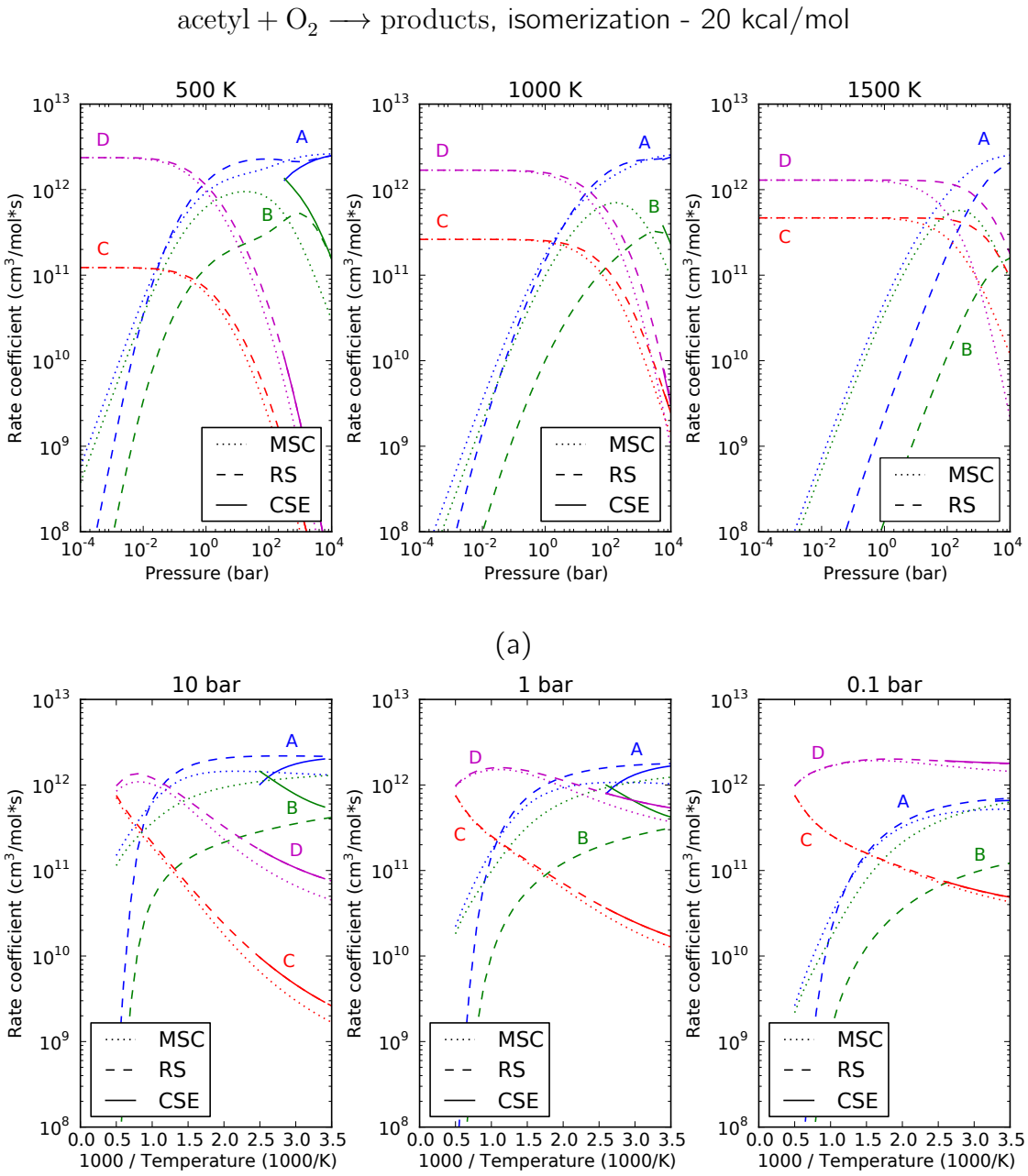

Figure 26: Comparison of rate coefficients versus (a) pressure and (b) temperature for $CH_3CO + O_2 \rightarrow$ products estimated using the modified strong collision (MSC), reservoir state (RS), and chemically-significant eigenvalue (CSE) methods for the acetyl + oxygen system with the isomerization transition-state barrier artifically decreased by 20 kcal/mol. In the plots, A = acetylperoxy, B = hydroperoxylvinoxy, C = ketene + HO_2, and D = lactone + OH.

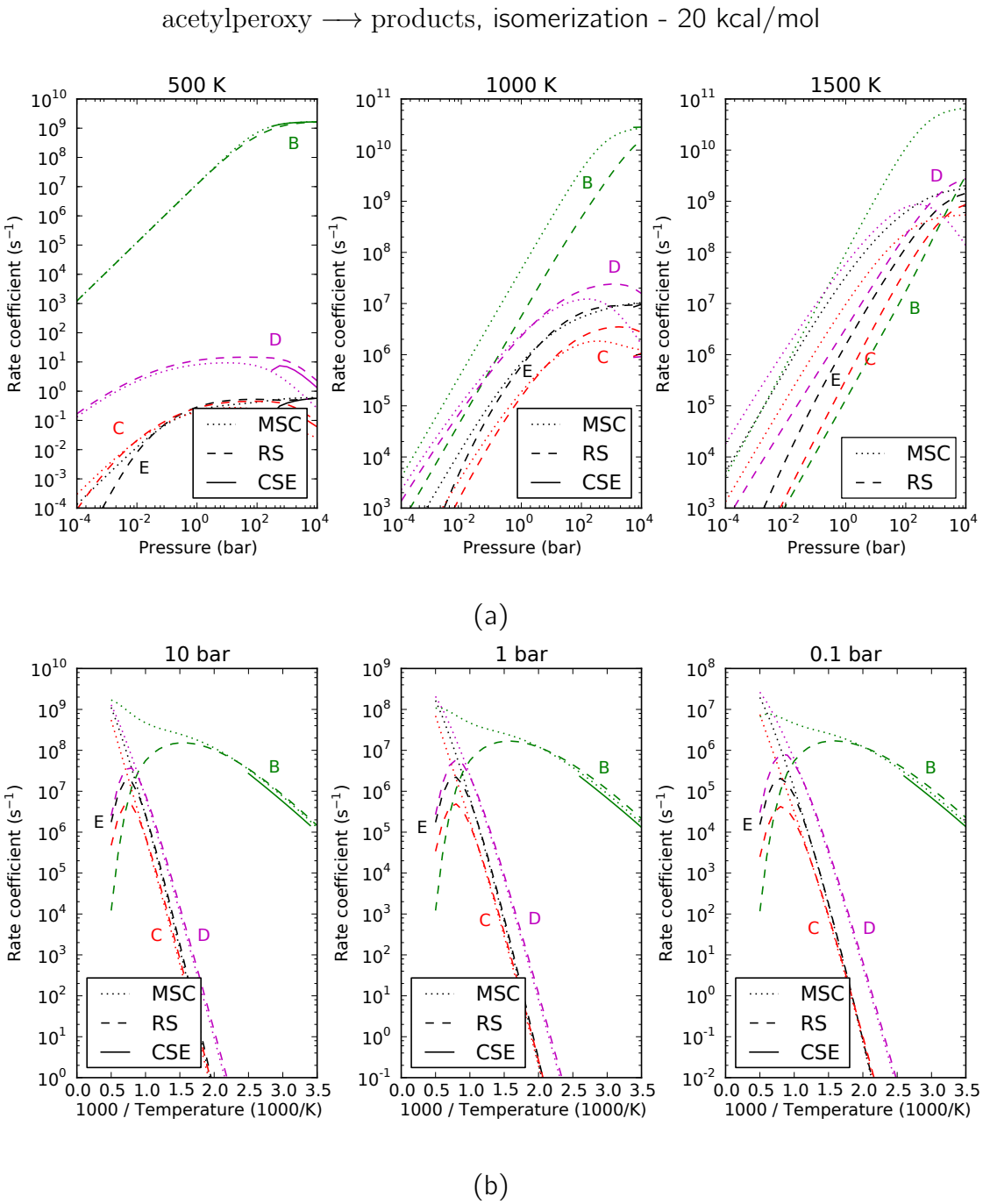

Figure 27: Comparison of rate coefficients versus (a) pressure and (b) temperature for $CH_3C(O)OO \rightarrow$ products estimated using the modified strong collision (MSC), reservoir state (RS), and chemically-significant eigenvalue (CSE) methods for the acetyl + oxygen system with the isomerization transition-state barrier artifically decreased by 20 kcal/mol. In the plots, B = hydroperoxylvinoxy, C = ketene + HO_2, D = lactone + OH, and E = acetyl + O_2.

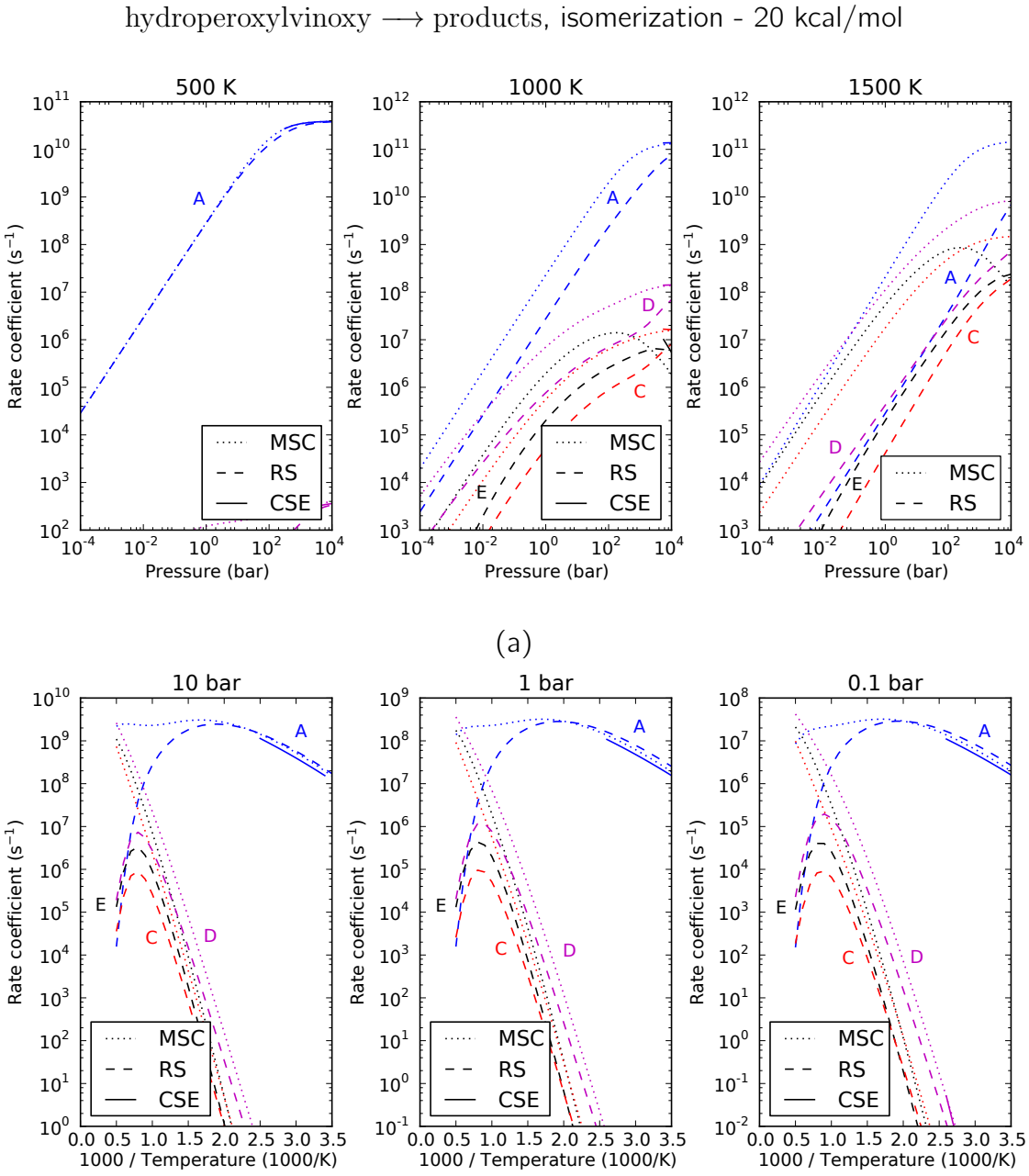

Figure 28: Comparison of rate coefficients versus (a) pressure and (b) temperature for $CH_2C(O)OOH \rightarrow$ products estimated using the modified strong collision (MSC), reservoir state (RS), and chemically-significant eigenvalue (CSE) methods for the acetyl + oxygen system with the isomerization transition-state barrier artifically decreased by 20 kcal/mol. In the plots, A = acetylperoxy, C = ketene + HO_2, D = lactone + OH, and E = acetyl + O_2.

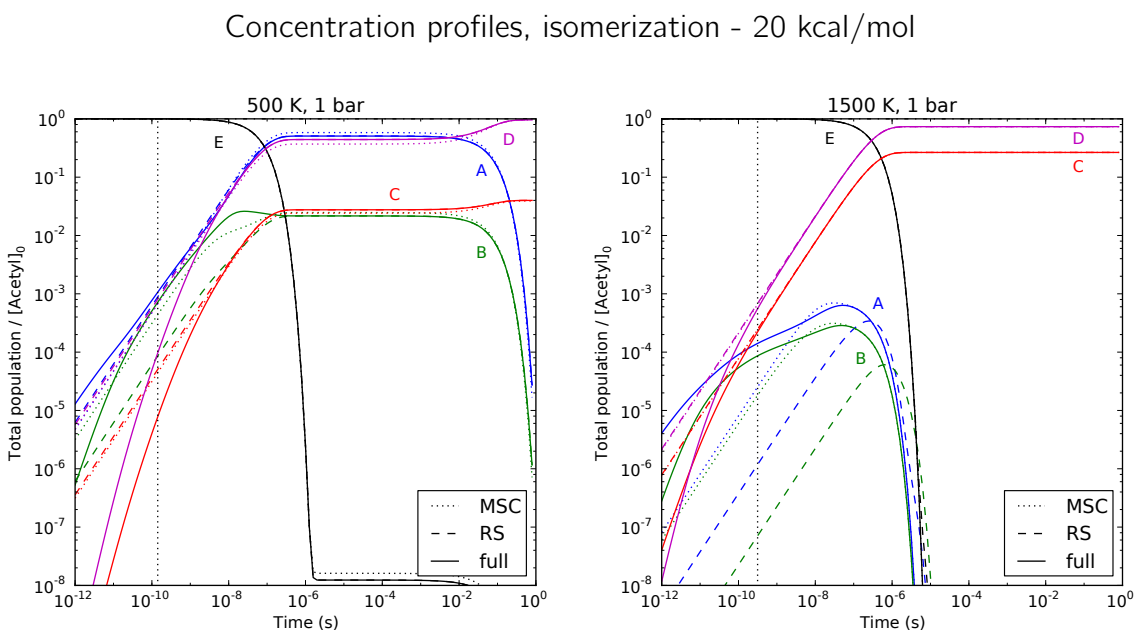

Figure 29: Concentration profiles at low-temperature and high-temperature conditions, comparing the modified strong collision (MSC), reservoir state (RS), and chemically-significant eigenvalue (CSE) methods with the full master equation solution for the acetyl + oxygen system with the isomerization transition-state barrier artifically decreased by 20 kcal/mol. In the plots, A = acetylperoxy, B = hydroperoxylvinoxy, C = ketene + HO_2, D = lactone + OH, and E = acetyl + O_2.